Proceedings of the International Conference on Creationism

Volume 9
Print Reference: 11-65

Article 31

2023

Craters and Cracks Caused by Accelerated Nuclear Decay Heat Throughout the Solar SystemAccelerated Radioactive Decay Heat in the Solar System and its Implications for Earth

Don Stenberg Jr.
N/A

Recommended Citation
Stenberg, Don Jr. (2023) "Craters and Cracks Caused by Accelerated Nuclear Decay Heat Throughout the Solar SystemAccelerated Radioactive Decay Heat in the Solar System and its Implications for Earth," *Proceedings of the International Conference on Creationism*: Vol. 9, Article 31.
DOI: 10.15385/jpicc.2023.9.1.5
Available at: https://digitalcommons.cedarville.edu/icc_proceedings/vol9/iss1/31

Stenberg, D. 2023. Craters and cracks caused by accelerated nuclear decay heat throughout the solar system. In J.H. Whitmore (editor), *Proceedings of the Ninth International Conference on Creationism*, pp. 11-65. Cedarville, Ohio: Cedarville University International Conference on Creationism.

CRATERS AND CRACKS CAUSED BY ACCELERATED NUCLEAR DECAY HEAT THROUGHOUT THE SOLAR SYSTEM

Don Stenberg, 695 Goodnight Hollow Rd. Walnut Shade, MO 65771, dnstnbrg@hotmail.com

ABSTRACT

Recently discovered thermal expansion cracks on the Moon and Mars can be best explained by an episode of major thermal expansion caused by accelerated nuclear decay (A.N.D.). Likewise the major volcanic flows of Mars (Tharsis volcanos) and the moon (lunar maria) are best explained by heat from A.N.D. Other phenomena such as the apparent resurfacing of Venus, excess heat from the gas giants, the transient Martian hydrosphere, the decay of the lunar magnetic field, the cryovolcanoes found on Pluto, etc. are also consistent with being caused by this pulse of decay heat. This same heat could have caused massive phreatic explosions on the rocky planets and moons resulting in crater formation. Early Creation Scientists believed that internal processes like volcanism formed the craters, and the uniqueness of 'impact signatures' has been overstated. Lunar craters associated with rilles, central peaks, and irregular mare patches are best explained as a phreatic explosion followed by significant lava flows. Mare lavas contain sufficient quantities of radioactive isotopes to cause the massive explosions needed to form the mare craters. Possible explosion mechanisms are considered, and the crater explosion hypothesis is compared with the crater impact hypothesis.

KEY WORDS

Accelerated radioactive decay, solar system, Mars, moon, thermal expansion cracks, craters, maria, Tharsis volcanoes

I. INTRODUCTION

Since Galileo first used a telescope to look carefully at the moon, scientists have wondered what processes caused the formation of the craters and maria. Over the last several decades, NASA's orbiters and landers have been able to return large amounts of detailed data and imagery not only of the moon but of many rocky planets and moons throughout the solar system. Many early creation scientists noted the similarities between the craters seen on the moon and the craters seen in volcanically active regions of the Earth, but lacking a volcanic mechanism capable of generating such voluminous craters, most scientists today believe that the craters were largely formed as the result of impacts. With the RATE project's discovery of significant evidence for at least one pulse of accelerated nuclear decay, we finally have the possibility of an internal energy source capable of generating the enormous craters we see on the moon and elsewhere. This paper will first begin with a comprehensive survey of evidence for the effects of heat from accelerated radioactive decay throughout the solar system (except for craters) and then will go into detail with reasons to believe that the craters may also be an effect of this same decay heat.

II. EVIDENCE FOR ACCELERATED NUCLEAR DECAY HEAT THROUGHOUT THE SOLAR SYSTEM

A. Major Thermal Expansion Cracks on the Moon and Mars

Recent NASA missions have given us more detail and more information about the Moon and Mars than we have ever had before. One of the most significant achievements has been their ability to create relatively detailed gravity maps of the Moon and Mars. Gravity maps can reveal important information about what sorts of structures exist below the surface of a planet, because density differences will show up as higher or lower gravity fields than would otherwise be expected. NASA's GRAIL (Gravity Recovery and Interior Laboratory) mission to the Moon used a pair of spacecraft, orbiting relatively near the lunar surface, to get an exceptionally clear picture (Figure 1) of its gravity field.

The large, straight blue cracks around the perimeter of the maria are not structures that could be produced by impacts, but instead appear to be thermal expansion cracks. As the interior of the Moon heated up rather suddenly, especially under the maria, the overlying cooler rock was stretched apart until it ruptured and these cracks formed and subsequently filled with lava (Zuber et. al., 2014). The lava has been enriched in radioactive elements like Thorium, Uranium, and Potassium-40 compared to the rest of the rocks found on the Moon. Apparently, the near side of the Moon was created with a higher inventory of radioactive isotopes than the far side, which would be why the near side has large lava flows while far side is largely devoid of lava-filled craters. (Figure 2, Figure 3) This asymmetry may also be associated with Earth's gravity similar to a single tidal motion as the moon heated and plastic deformation occurred.

Maria Zuber, MIT's Vice President for research and a leader of the team that analyzed the data said about the source of heat that caused the cracking, "It could be due to radioactive decay of heat-producing elements in the deep interior….People who thought that all this volcanism was related to a gigantic impact need to go back and think

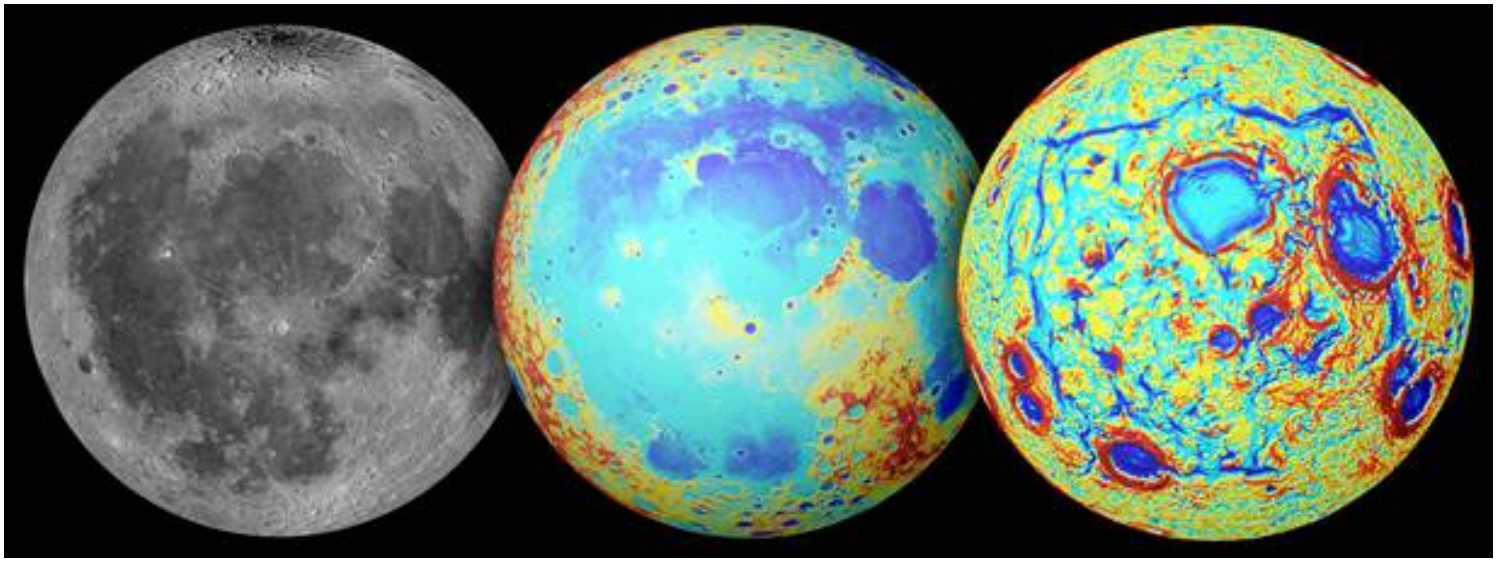

Figure 1. Moon as seen from Earth (left); the topography of the Moon (center); GRAIL's gravity map of the Moon, showing huge blue cracks, forming roughly a square around the lunar maria (right)

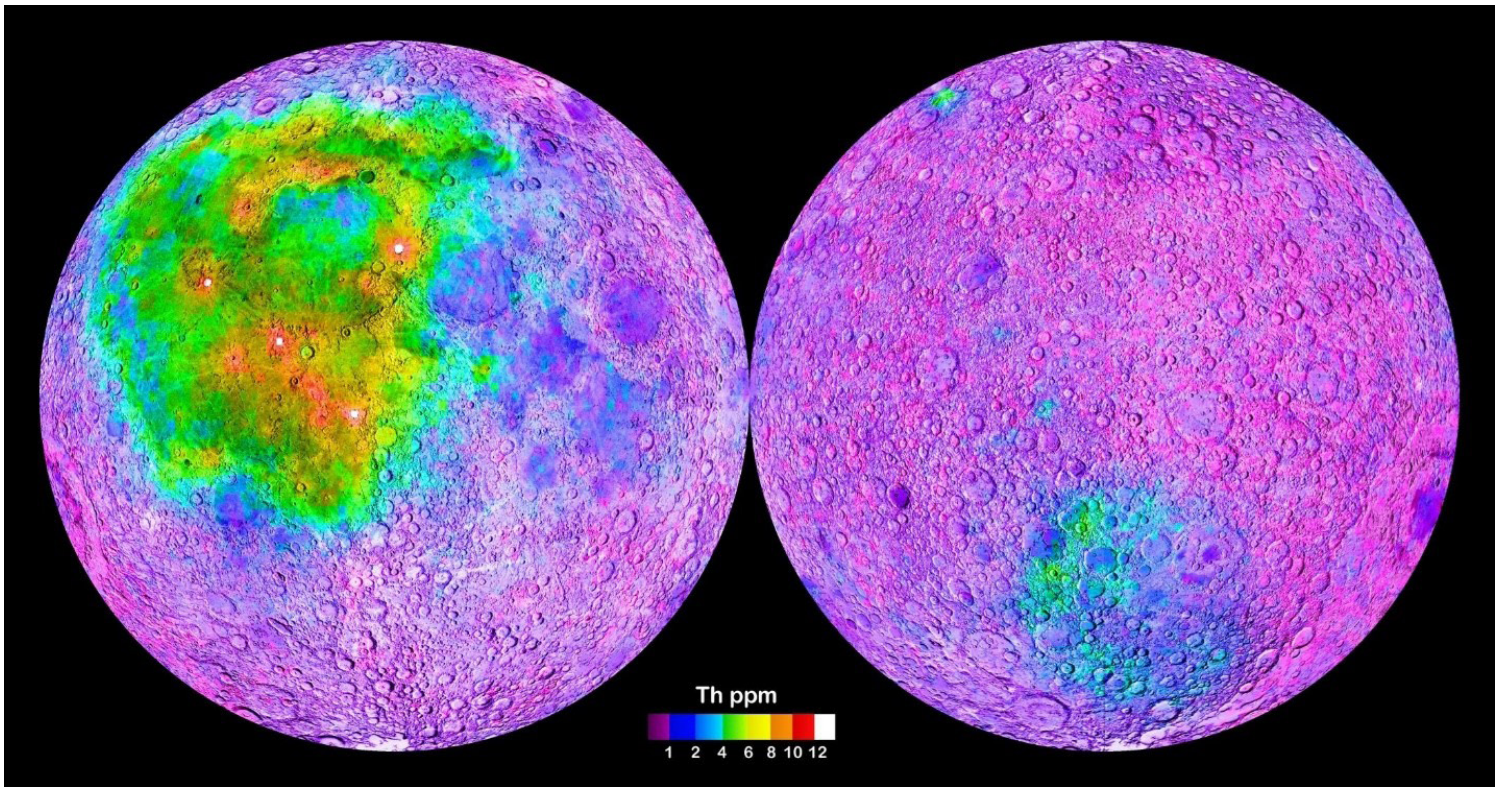

Figure 2. Thorium map of the Moon showing increased concentrations of Thorium in the main maria regions on the near side (left). These lavas apparently became enriched in mantle incompatible elements while they melted, causing further heating of the magmas and contributing to the thermal expansion cracking around the perimeter of the maria.

some more about that" (Chu, 2014). Ian O'Neill writing for Discovery News summarized the findings, saying of the lava-filled cracks "researchers have found compelling evidence that it was formed in the wake of a mega volcanic eruption and not the location of a massive asteroid strike" (O'Neill, 2014). For the thermal expansion cracks to form, the heat has to be generated inside the moon much faster than it can be conducted out to the crust of the moon. Slow and gradual nuclear decay over billions of years would not result in thermal expansion cracks, since the heat would have time to become relatively evenly distributed between the interior and the crust over such a timescale. Nor would slow and gradual heating account for the very large quantities of lava that filled these cracks. So these secular scientists remained puzzled at these findings.

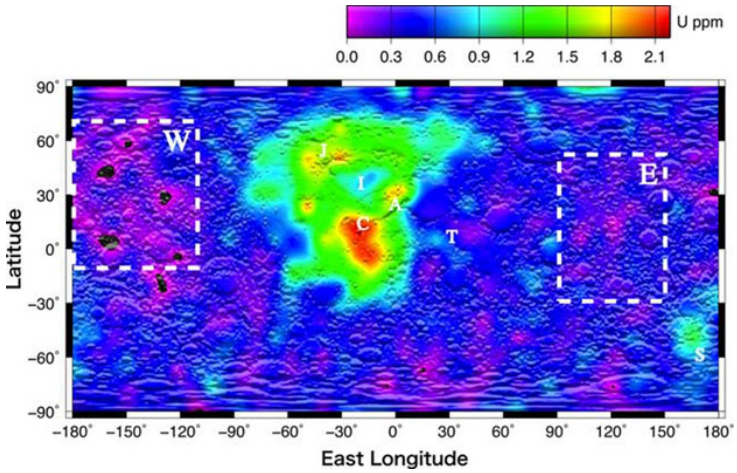

Figure 3. Uranium map of the Moon showing that the maria are likewise enriched in Uranium

If, as seems to be the case with the Earth (Stenberg, 2012), the Moon was initially created to be cool throughout and was heated by radioactive decay to its current internal temperature, we can calculate the amount of thermal expansion that it would experience, and we can compare the increased circumference to the overall size of the thermal expansion cracks. Although it's hard to exactly measure the width of the cracks, it appears as though the total circumferential expansion of the Moon was approximately 200 km. Using this figure, the total radial expansion of the moon would have been about 32 km, which would require an increase of the average internal temperature of the Moon of about 1000 K. This corresponds to approximately three quarters of all radioactive decay heat that would have ever been produced on the Moon, assuming the equivalent of 4.5 billion years of decay. (Appendix A) This heat pulse needed to occur fast enough inside the Moon so that the lunar crust was not able to thermally expand to the same degree as the interior due to conductive heat transfer from the interior. The lunar maria basalts are relatively enriched in radioactive materials such as Uranium and Thorium compared to the rest of the lunar crust, meaning that a disproportionate amount of the heating would have taken place deeper inside the moon. If all 4.5 billion years of decay equivalent occurred in one year-long event, then the other 25% of the heat would have to be accounted for. One possibility is that some of this missing heat escaped the interior of the moon when volcanic explosions blasted molten materials and water vapor into space around the Moon where they could have cooled more quickly due to radiative cooling. Some of those materials would have re-fallen to the lunar surface as regolith, ice, or even small meteorites. Another possibility is simply that the assumptions that were made in arriving at the total inventory of radioactive isotopes on the moon that are being relied on for this calculation resulted in a value that is 25% different than the actual value. Finally, it is also possible that 200 km of circumferential expansion is a slight overestimate. However, even a 75% match between decay heat and heat needed to thermally expand the moon to its present size is quite close given the uncertainties in some of the values used in the calculations.

The situation appears similar on Mars. Its gravity map shows a number of large cracks to the east of the Tharsis region – the region that contains Olympus Mons and the three other prominent Martian volcanoes which lie is a line from northeast to southwest. Most of the cracks are largely filled in on Mars, too, with the major exception of Valle Marineris, the largest canyon in the solar system by far. (Figure 4) Although some have proposed that this canyon was carved by water, it is a local minimum in elevation, and it appears as though it would receive incoming water from any direction with no obvious outflow that would enable a megaflood to carve it. This is unlike the Grand Canyon, for instance, which has a downward pitch that allows the Colorado River to keep flowing, eventually to the Gulf of California. So a better explanation is that there was some kind of internal heating event for Mars that caused the interior to expand relative to the crust, leading to the formation of this series of thermal expansion cracks and also to the relatively rapid formation of these Tharsis volcanoes – among the largest in our solar system. Indeed, other creation scientists have already proposed that many of the features on Mars can be explained by a period of accelerated radioactive decay (Samec, 2014).

If, as we did for the moon, we assume that Mars was initially created cool throughout and the heat from accelerated nuclear decay heated it to its current temperature, we can again compare the change in size, inferred by the size of these cracks, to the amount of thermal expansion we would predict from the heat of accelerated nuclear decay. It appears that adding the width of Valle Marineris with the other cracks discovered by its gravity mapping mission yields an approximate increase in the Martian circumference of about 400 km, which implies a radial expansion of about 64 km. This would require an increase of the average internal temperature of about 1400 K, which would have required about 90% of all the radioactive decay of Uranium, Thorium, and Potassium-40 that would have occurred over the equivalent of 4.5 billion years to have occurred in one relatively rapid event. Perhaps the other 10% would have radiated into space as the lavas that formed Olympus Mons and the other Tharsis volcanoes cool radiatively in the thin atmosphere (Appendix B), or perhaps the real value is 10% different than the one used in this calculation, or perhaps 4.5 billion years equivalent is off by a similar small percentage. In any case, it is significant that the calculated values for heat needed for thermal expansion are quite close to the calculated heat released in an accelerated nuclear decay event.

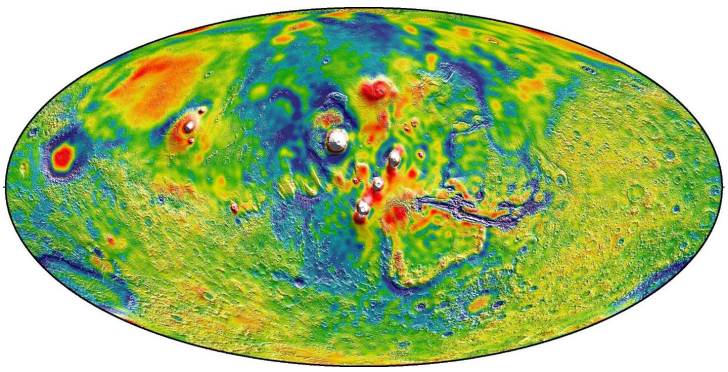

Figure 4. Gravity Map of Mars showing a series of fairly straight cracks that have mostly been filled in. Note that Valle Marineras, the largest canyon in the solar system, appears to be connected to the other apparent cracks, but is not filled in.

So we see that these thermal expansion cracks add additional evidence to the effects of accelerated nuclear decay that must have occurred after the Day 4 creation of the Moon and Mars. The approximate temperature change can be inferred from the increase in circumference implied by the size of these thermal expansion cracks, and the temperature change needed is quite similar to the temperature change that would take place in a single pulse of approximately 4.5 billion years equivalent of accelerated radioactive decay.

B. Major Volcanic Activity on the Moon and Mars

There is evidence of a massive amount of volcanism that has taken place since the initial formation of the planets and moons, all of which required significant energy. On the Moon, approximately 16% of the surface is covered with massive basalts that Galileo mistakenly named "seas" or "maria". (Figure 5) These massive eruptions require a massive amount of heat to melt and transport all of that material from the lunar mantle to the surface – approximately $5.4*10^{25}$ Joules to heat and melt all of the lava that fills the maria, according to these authors' calculations. The most common hypothesis for how these maria formed is that there were huge impacts to form the "impact basins" on the moon, and that the energy from these huge collisions cracked the underlying rock and/or heated it up to the point of melting so that as a direct consequence of the mega impact, these massive volumes of lava came to the surface and filled the massive craters caused by these impacts. However, as we have already noted, the discovery of the thermal expansion cracks all around the perimeter of the maria strongly implies that the source of the heat to melt the lava was internal to the Moon, such as accelerated radioactive decay. Therefore the existence of extensive volcanic flood basalts on the Moon is another example of the heat from radioactive decay causing massive geological events to occur beyond the Earth at some time after Creation Day 3. Incidentally, all that is needed to explain the uneven maria distribution on the Moon is simply an initially non-uniform distribution of radioactive isotopes in the lunar mantle.

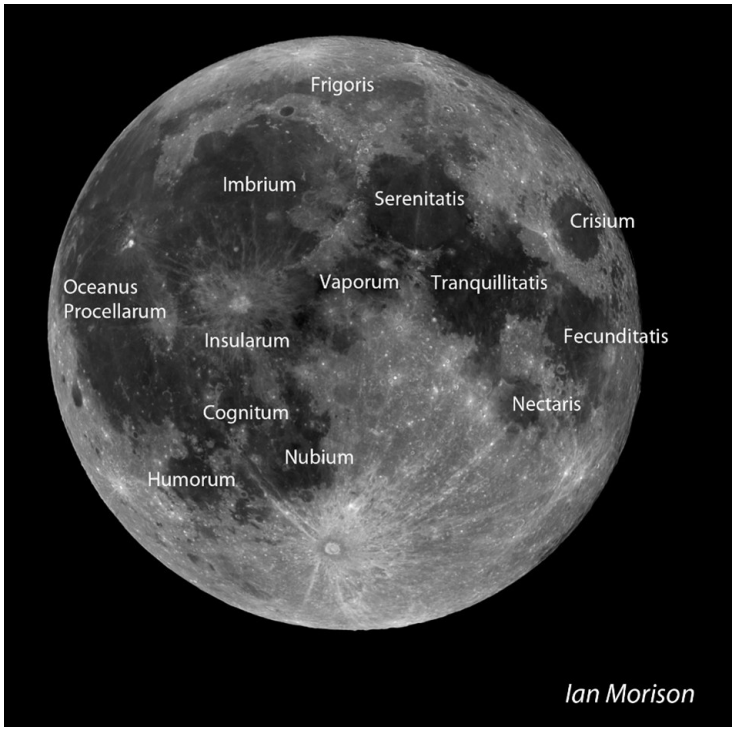

Figure 5. Lunar Maria

Some of the largest volcanoes in the solar system are found in the Tharsis region of Mars, near Olympus Mons. (Figure 6) These volcanoes deposited huge amounts of ash in that region (Hynek et. al., 2003). The entire region is considered to be volcanic in origin, and volume of the volcanic rock in the Tharsis region has been calculated to be approximately 10^{21} kg (Phillips et. al., 2001), (Nimmo & Tanaka, 2005). To heat and melt that much material would require an enormous amount of energy – approximately $2.5*10^{27}$ Joules. Within a Young-Earth paradigm, the most likely source of that heat is again accelerated radioactive decay, especially considering the cracks on Mars that are most likely the result of its thermal expansion. And the Tharsis volcanoes are clearly not impact structures but instead clearly resemble shield volcanoes on Earth. This heating must have occurred no earlier than Creation Day 4 when Mars was made and could have occurred during the Flood on Earth.

Another interesting feature of Mars is that the entire Tharsis region sticks out so far from the Martian surface and it is a high gravity anomaly. If Mars' mantle was sufficiently warm during and after the eruptions that it would plastically deform, then the Tharsis region would be in isostatic equilibrium. But if the Tharsis region was in isostatic equilibrium, it would have a lower than average density given its volume. However, its gravity implies a density similar to the rest of the crust. This strongly implies that much of the mantle that it rests upon was solid and relatively cool during the eruption phase. This is consistent with the hypothesis that Mars was created cool throughout, and that an initially inhomogeneous mantle-distribution of radioactive isotopes caused only a portion of the lower mantle to melt during accelerated decay and erupt as a massive volcanic region, leaving most of the mantle cool enough to support the added weight of the lava without plastically deforming.

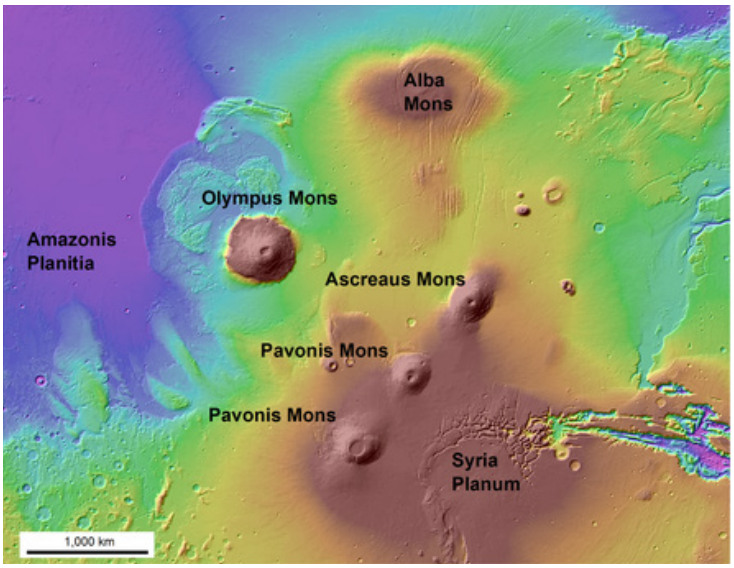

Figure 6. Topographic Map of Mars' Tharsis Region

C. Other Solar System Phenomena Consistent with Heat from Accelerated Nuclear Decay

1. Small Shrinkage Escarpments on the Moon and Mars still causing earthquakes

NASA's Lunar Reconnaissance Orbiter photographed thousands of small escarpments, which appear to be folds in the lunar crust caused by the shrinking of its interior. Seismometers left on the moon by the Apollo missions detected shaking that is probably the result of the continued shrinking of the interior, crustal movement, and building up of some of these escarpments. After the major thermal expansion cracks formed and filled with lava that solidified, the interior of the moon began slowly cooling, and thereby slightly shrinking in size over time. (Steigerwald, 2019) That these escarpments are still forming today strongly implies that the moon is not in thermal equilibrium, and that its interior is hotter than would be the case if it was really 4.5 billion years old and there had been no period of accelerated nuclear decay.

2. Resurfacing of Venus

The surface of Venus is obscured by its continual global cloud cover, but its surface features can be seen using radar. NASA's Magellan mission mapped the surface in high resolution several decades ago. Scientists were surprised to find that its surface is nearly free of craters, which has led many to conclude that at some relatively recent time, the entire planet was resurfaced in a rapid global tectonic event (Strom et. al., 1994). Creation scientists have proposed that the heat energy needed to drive such an event came from accelerated decay (Baumgardner, 2002). Due to the cloud cover and extreme temperatures, it has been hard to get detailed data on the global distribution of radioactive isotopes, but gamma ray spectrometers on the Venera landers gave readings that imply a similar concentration of Uranium, Potassium, and Thorium to terrestrial basalts or other volcanic rocks (Taylor et. al., 2018). (Figure 7)

Since Venus is similar to the Earth in size and composition, it seems reasonable to assume that calculations done for the energy balance of accelerated radioactive decay on Earth (Stenberg, 2012) would be similar to the heat balance on Venus. Likewise, it seems likely that similar processes of crust-mantle differentiation and enrichment of the crust with radioactive isotopes would have taken place. One key difference, though, is that Venus has very little water, which would have affected its ability to reject decay heat from its surface, and also would have impacted the melting point of its mantle and crust materials. Regardless, the present surface of Venus implies that the majority of heat associated with accelerated decay went into heating the interior of the planet and causing global, catastrophic geological effects, and that it occurred after the creation of Venus on Creation Day 4.

3. Gas Giant Heat Balances

Most of the gas giants are emitting more heat from their surface than they are receiving in light from the sun. (Samec, 2000). This implies one of two things. One of these is that there has been and still is a relatively small internal continuous heat source of some kind. The alternative is that in the fairly recent past there was a pulse of heat and what we are seeing is the remnants of that heat pulse. The most likely source of this pulse of heat would be from accelerated radioactive decay, as discussed herein.

4. Transient Martian Hydrosphere

Due to its lower gravity and weak magnetic field, Mars seems incapable of retaining an atmosphere for long. However ample evi-

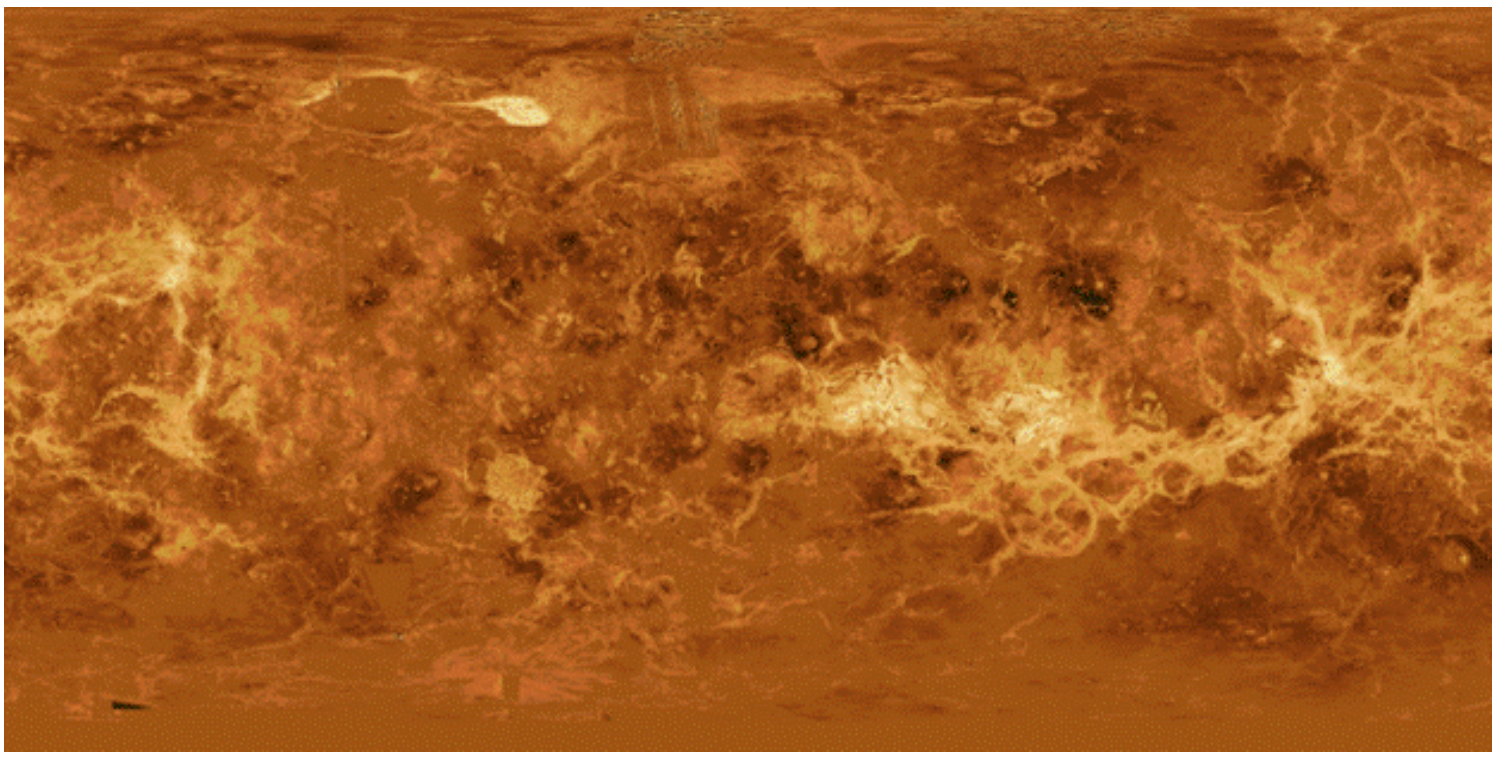

Figure 7. Global map of Venus showing a dearth of large impact craters, implying a relatively recent resurfacing event

dence has been found for large-scale watery erosion and deposition on Mars (Zuber, 2018), including river deltas consistent with rivers running for less than 2,000 years. Perhaps the same heating event that cracked the crust and formed the massive volcanoes also melted and released enough water vapor to create an atmosphere to produce rain and catastrophic flooding on Mars (Samec, 2014). Planets and moons with weaker gravity than Mars, such as the Moon and Mercury, would not have been able to retain a viable atmosphere long enough for liquid water to produce similar effects on their surfaces.

5. Cryovolcanism on Pluto

The recent flyby of Pluto by NASA's New Horizons spacecraft surprised secular scientists when they discovered evidence of recent cryovolcanism on its surface. So far from the sun, and so many billions of years after they believed it formed, there should not have been enough heat retained within Pluto to enable cryovolcanism. Again, a pulse of accelerated radioactive decay could supply this energy.

6. Decay of Lunar Magnetic Field

There is a notable correlation between the decline of the magnetic field of the moon as measured in the remnant magnetization of surface rock and the radioisotope "age" of those rocks (Humphreys, 2014). If there was an independent way to measure how much the rate of radioactive decay was increased, we could determine how fast the magnetic field decayed. Fortunately, the formation of radiohalos on Earth gives us an approximate measure of decay acceleration, approximately 10 to 20 million years' equivalent per day, or 4.5 billion years equivalent in roughly one year (Stenberg, 2012), if the same decay pulse the affected the Earth also affected the rest of the solar system. In this scenario, it appears as though the decay of the moon's magnetic field occurred during the space of only one year or so. Such a rapid decay would require a massive heating event that heated and melted the core, and also generated enough turbulence inside the lunar core to not only generate what appear to be extreme, two order of magnitude swings in the magnetic field strength (Humphreys, 2014), but also cause enough turbulence such that the induced electrical current decayed relatively quickly. Using an estimate of present core turbulence intensity will underestimate this. Secular researchers studying the data from Japan's SELENE lunar mission were indeed surprised to discover evidence that there remains to this day a very soft or molten layer near the moon's core (Harada et. al., 2014), which is consistent with the hypothesis that it heated and melted recently, since it has not yet had time to fully cool off.

7. Isotope Ratios and Fission Tracks on Lunar Rocks are Evidence of Radioactive Decay

Lest someone postulate a different energy source for this apparent pulse of heat on the moon and elsewhere, it should be pointed out that the rocks we returned from the moon and analyzed contained ratios of parent and daughter isotopes that are consistent with about 4.5 billion years of total nuclear decay equivalent on the moon. Furthermore there were some fission tracks found in some lunar rocks, which is again consistent with actual nuclear decay having taken place on the moon, since spontaneous fission is one common form of radioactive decay and would likely also have been accelerated along with alpha and beta decay.

D. Implications of Heat from Accelerated Nuclear Decay Throughout the Solar System

1. As noted above, the thermal expansion cracks of the moon and Mars give us a means to estimate the total thermal expansion of those bodies in a relatively short period of time, sometime on or after Creation Day 4, and the amount of heating needed is remarkably close to the amount of heat generated by the equivalent of 4.5 billion years worth of nuclear decay of the radioactive isotopes on those worlds. The large-scale volcanism of those worlds lends further weight to the idea that a large amount of internal heating has taken place there. And several other phenomena in the solar system are also consistent with that hypothesis.

2. One final major feature of the rocky planets and moons still needs to be considered: could the ubiquitous craters in the solar system have also formed as a result of internal heating caused by accelerated nuclear decay? Maar craters on Earth were formed by steam explosions and can reach over 5 km in diameter. The basic cause of these explosions is the right combination of heat, pressure, and a volatile substance that can very quickly change from a supercritical fluid or liquid to a gas. On Earth, for acknowledged maar craters, this substance is usually water. The pressure is due to the weight of the overlying rocks. So as this heated water makes its way toward the surface, at some point the pressure from the overlying rocks becomes just slightly less than the vapor pressure of the water. Once the top of that pocket of water crosses this line, the entire pocket will flash to steam almost instantaneously. The amount of hot fluid will determine the size of the explosion and subsequent crater. How big could maar craters get? If there is a sufficient quantity of hot, pressurized, supercritical water, heated by a pulse of accelerated radioactive decay, could even the largest craters in the solar system have been formed by steam explosions?

III. CRATER FORMATION A RESULT OF ACCELERATED NUCLEAR DECAY

A. History of the Crater Debate

1. Most Early Creation Scientists Believed In A Volcanic Origin of Craters

Most early scientists (who were almost all creationists and believed in a global Flood) believed that the craters on the moon and elsewhere were formed by internal, volcanic-type processes. One of the first scientists to consider the origin of the moon's craters, Robert Hooke, writing in the 1600s, considered the possibility of an impact origin. He believed that a volcanic origin made more sense after he observed that boiling alabaster produced crater-like formations, also akin to volcanic craters (Hooke, 1665). Most scientists for the next 200 years agreed with his view that the craters had a volcanic origin, an opinion strengthened by periodic reports of molten lava visible on the surface of the moon (Shoemaker, 1962). The list of names of scientists believing the craters to be volcanic in origin is long: Astronomer William Herschel, his son Astronomer Sir John Herschel, Selenographer J. F. Julius Schmidt, Geologist J. Elie de Beaumont, Volcanologist G. Scrpoe, Geologist James Dwight Dana, Royal Astronomical Society Fellow Edmund Neison, Geophysicist Stjepan Mohorovicic (son of Moho Discontinuity discoverer Andrija Mohorovicic) are a few of these. Sir John Herschel noted the strong

similarity between the volcanic craters in the Campi Phlegraei in Italy and the craters on the Moon. Edmund Neison published a book on the Moon favoring the volcanic hypothesis for crater formation in the 1870s (Hoyt, 1987).

Speculation on the mechanism of crater formation continued with the publication of The Moon: Considered as a Planet, a World, and a Satellite by James Nasmyth and James Carpenter in 1874, which considered a number of possible volcanic mechanisms. Nasmyth and Carpenter did consider the possibility of steam explosions, but they noted that the apparent lack of water on the moon made it difficult to see how that could account for the "immense display of volcanic action which the surface exhibits". However, a recent reanalysis of rocks returned from the moon has indeed found some trace amounts of water, not much, but potentially enough to make a difference geologically. Furthermore, since they assumed that the Moon had accreted over time from a primordial nebula and initially was a molten ball, they said "it does not appear clear how expansive vapours could have lain dormant till the Moon assumed a solid crust, as all such would doubtless make their escape before any shell was formed, and at an epoch when there was ample facility for their expansion". However, if the Moon was initially created cool, this objection does not apply. These authors also considered the possibility of underground explosions, especially since the craters are mostly perfect circles. But they didn't have a way to explain "such a very local generation of a deep-seated force" and even if they did, they didn't see how an explosion would produce raised crater walls (Hoyt, 1987). But circular maar craters up to several kilometers in diameter are known to form on earth due to steam explosions that originate underground. Also, subterranean nuclear explosions have shown that raised crater rims do form from such explosions, and the physics involved is now understood. So, neither of those objections seems any more to be very convincing.

Grove Gilbert worked for the US Geological Survey and had the chance to visit Barringer Crater, which he concluded was formed as a maar volcanic crater after failing to find any magnetic evidence for a large amount of buried iron in the crater, and after calculating that the volume of material in the rim matched the volume of the hole. He also considered the formation of lunar craters, and believed that the smaller craters may have likewise been maar craters, but he couldn't imagine that a similar process could form craters on the moon with over a hundred of times larger diameters than most maar craters formed recently on earth (Hoyt, 1987). However, he knew neither about evidence for immense thermal expansion cracks nor for accelerated radioactive decay, including how much energy would have been available to cause enormous craters during such an episode.

Indeed, the question of how lunar craters could be so large compared to any known terrestrial examples was a frequent objection to volcanic cratering hypothesis, particularly from the 1800s and beyond. A likely reason for this objection is that, by this time, the doctrine of uniformitarianism was gaining scientific respectability, and craters that are over 1000 km in diameter such as are seen on the moon are wildly inconsistent with slow and gradual geologic processes over the ages, particularly if they are due to internal forces on the moon. For instance, Ralph Baldwin reasoned that volcanic processes that produced craters of a maximum size of only a few kilometers in diameter in recorded history, such as Tambora in 1815, could not explain lunar craters that are sometimes over 1000 km in diameter (Spudis, 2010). In a sense, he was right. Craters that large would require many orders of magnitude more heat and energy than are available today, such as the heat produced by accelerated radioactive decay. If they were fully aware of the massive volcanoes on Mars and the giant thermal expansion cracks on the moon and Mars, and the energy required for their formation, would they have been so quick to reject volcanism as a cause of many of the craters on the Moon?

2. "Impact Signatures" Reconsidered

A number of features have been proposed to be impact signatures, or features that allegedly can only be explained by an asteroid or cometary impact but not by a volcanic explosion. Some of those proposed features include shock metamorphism, planar deformation features, shatter cones, and impact melts (Grieve et. al., 1996). The impact theory states that these features form only under the extremely high transient pressures of the shock of a high speed impact. However, every one of these features is also present in underground nuclear explosions, as in the Sedan nuclear test crater and other craters formed by nuclear explosions. (Figure 8). So these features are not necessarily impact signatures, but rather signatures of high energy explosions that generate high local pressures more generally. So it is not clear from a physics standpoint why an impact-induced explosion with enough energy to form a 2-km diameter crater would generate a substantially higher shock pressure than a volcanically-induced steam explosion with enough energy to form a 2-km diameter crater. Indeed, alleged impact signatures need to be tested by systematically surveying every similar maar crater for "impact signatures" such as shock metamorphism and shatter cones. If some impact signatures are found at some clear maar craters such as MacDougal and Elegante craters in the El Picante volcanic field in Mexico near the Arizona border, then it needs to be admitted that these are not impact signatures at all. Indeed, it is a prediction of this hypothesis that some "impact signatures" will be found at some of these maar craters

Figure 8. Sedan Nuclear Test Crater

if a comprehensive survey is completed.

Dr. Tim Clarey has recently published an excellent article analyzing the Chicxulub site (Clarey, 2017). Dr. Clarey notes that reports of planar deformation features (PDFs) have been found in "samples from the Toba volcanic caldera, Indonesia", citing Alexopoulos, Grieve and Robertson (Alexopoulos et. al., 1988). Clarey, citing another paper by Huffman and Reimold (Huffman & Reimold, 1996), states that they "described several conditions where the development of over-pressured conditions in the magmatic systems were sufficient to create PDFs, including quench supersaturation, catastrophic phase changes and gas-phase explosion. Under the right conditions and the presence of explosive gases, catastrophic gas reactions can contribute to a propagating, shock-induced wave front. Most of the shock-generating conditions described by Huffman and Reimold involve rapid ascent and rapid crystallization of magmas, which seem to be much more common than petrologists once believed". The volcanic explosion of Mount Tavurvur in 2014, caught on video, seems to be another example of this kind of shockwave inducing explosion. So it seems that any feature that can be produced in either an impact or a terrestrial volcanic explosion cannot be considered to be an impact signature in a way that rules out volcanism.

Another feature of some craters that has been put forward as explicable only with the impact hypothesis is the system of rays found along some craters. It is believed that they are the result of ejecta being explosively launched in all directions around an impact. However, underground nuclear explosions like Sedan have also produced ejecta blankets similar to both volcanic explosion craters like Mt. St. Helens and also some alleged impact craters like Barringer Crater. Indeed, in the video of the Sedan nuclear test, there are large chunks of debris leaving trails of dust through the air. On Earth, these chunks and clouds of debris encounter significant gravity and air resistance which prevent them from forming ray structures as large as those seen on the moon. So one way to test this hypothesis would be to bury a nuclear explosive on the moon and see what sort of crater and ray system it produces. This paper's hypothesis predicts that it would for a crater pattern similar to those seen in other well preserved lunar craters.

It has also been argued that steam explosions and meteorite impacts will operate in different temperature ranges. However, since equivalent amounts of energy are needed to produce equivalently sized craters, it is not clear why that should be the case. Furthermore, since (as argued above) impact explosions and volcanic explosions produce similar geological features, this is prima facie evidence that they also operate in similar conditions including similar temperature ranges. It seems that more work needs to be done modeling the conditions at the heart of a steam explosion now that we have computers capable of such simulations, but based on observed effects, it seems likely that such work would reveal some very high velocity impacts and also high temperatures caused by the explosion energy.

Furthermore, there are some features on Earth that appear to have been caused by an impact or other high energy explosion, but that lack almost all of these alleged impact signatures. One notable example is the Hudson Bay Arc, also known as the Nastapoka Arc, shown below (Figure 9).

Clearly the Hudson Bay Arc forms nearly half of an almost perfect circle. Despite several attempts to find impact signatures associated with this land form, none have ever been found. Features like this one place proponents of the impact theory on the horns of a dilemma. Either this is an impact crater, but the alleged impact signatures are not present, meaning that they are not impact signatures at all, or this is a crater formed by a volcanic explosion so massive that it caused a crater over 450 km in diameter, in which case even the largest of the lunar craters could also be the result of volcanic explosions. Neither scenario bodes well for the impact hypothesis. Are there any unambiguous signatures of impacts after all?

3. Barringer Crater Re-examined

Since Barringer Crater, also known as Meteor Crater, figures so prominently in the history of the development of the impact model, it is worth taking another look at the evidence that has been put forward that it is in impact crater and not a volcanic maar crater. If the evidence for an impact formation of Barringer is equivocal, then the entire case for the impact origin of craters throughout the solar system can be called into question. A survey of craters throughout North America has been undertaken, and many craters have been found that share very similar morphological characteristics with Barringer, despite arguments to the contrary. In size, shape, depth, and proximity to volcanic rocks exposed at the surface, Barringer fits in exceptionally well with a multitude of maar craters found throughout North America, as well as around the world.

As you can see, there is nothing immediate that stands out visually or topographically to make Barringer Crater obviously an impact crater whereas the others are undisputedly steam explosion craters, to which the label "maar" applies. Indeed, there are strong similarities. The diameter, depth, steepness of the sides, flatness of the bottom, and proximity to obvious volcanoes at the surface for Barringer are all in line with what we see for maar craters throughout North America.

Furthermore, maar craters generally need both groundwater and

Figure 9. Nastapoka Arc in Hudson Bay

Figure 10. Satellite View of Craters in Southwest North America

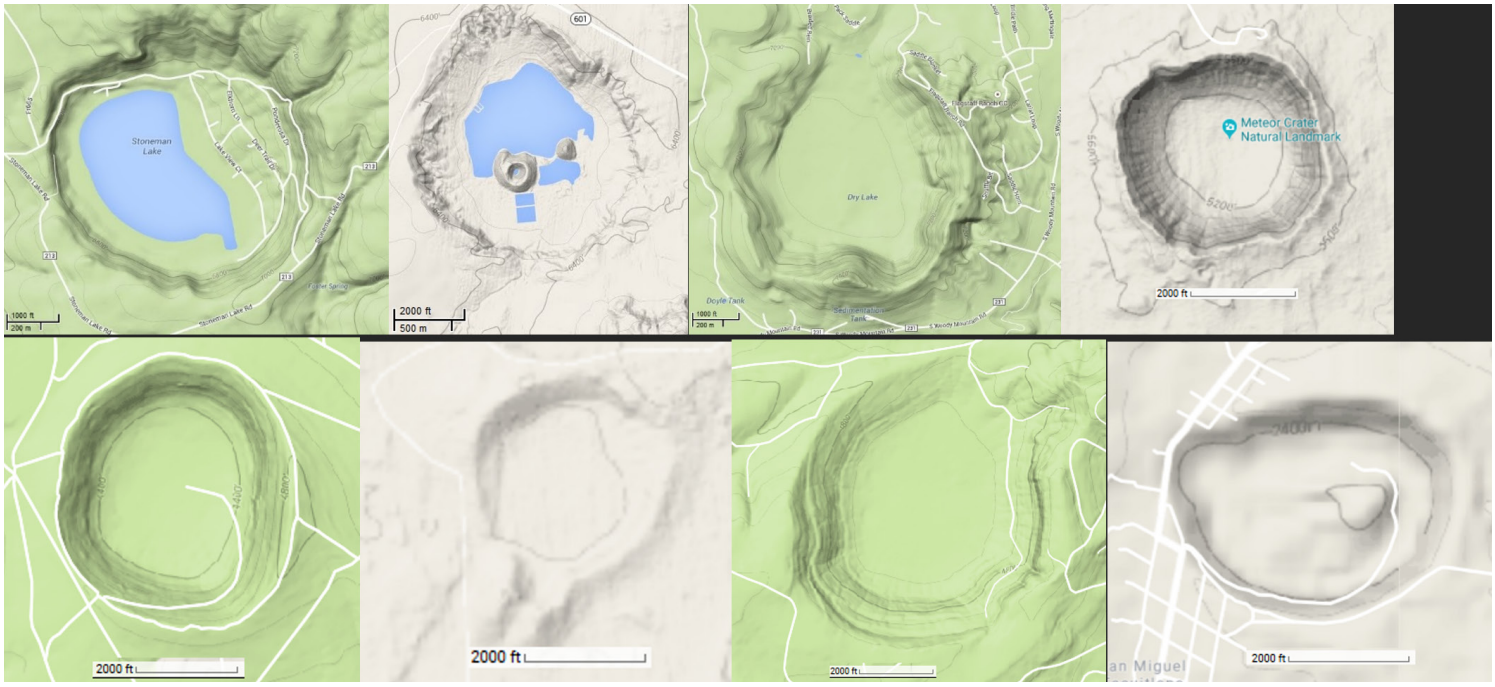

Figure 11. Topographic Maps of North American Craters

some sort of underground volcanic intrusion. There is still quite a bit of ground water in the region around Barringer Crater. In 2010 when a reading was last taken, the water level was 185 meters below the surface partway up the ejecta blanket, and about 150 meters below the surface a bit further away from the crater (Arizona Groundwater Site Inventory, 2018). Note that from underground nuclear tests, this explosion depth is consistent with the formation of craters like the Barringer Crater. In addition, there is a nearby volcanic range that appears to have emerged from a fissure whose end points straight at Barringer Crater. This fissure, or another similar one, may well continue underground in the direction of the crater and, if so, it may be the source of volcanic heat needed to flash the ground water to steam, thereby forming a maar crater. Indeed, the squarish sides of the crater have been attributed to the pre-existence of faults or cracks in the rock (King, 2017).

One of the evidences that has been used to argue for Barringer being an impact crater is the finding of many large and small pieces of iron that have been found all around the crater that appear to be pieces of the impacting meteorite. However, there is some evidence that there are bands of magnetite (iron) hundreds of feet underground in this area that were merely excavated, transformed by the heat and pressure, and then hurled by a steam explosion. One line of evidence in favor of this view is that a borehole drilled on the south rim into undisturbed terrestrial rock found a nearly 10-m thick layer of what was interpreted to be meteorite debris approximately 240 meters below the floor of the crater. However, since this borehole began on the rim into undisturbed terrestrial rock, a hole drilled straight down should not encounter any meteorite debris at that depth. Such debris would need to travel a few hundred meters through essentially solid rock. This rock may have partially fractured in place but would have approximately the same density as solid rock, as it lacks the voids associated with breccia that lower its overall density (King, 2017). So the best interpretation of this iron layer is that it formed with the rest of the rock in the area and is not related to the formation of the crater. Shoemaker was aware of this mystery but apparently did not consider the possibility that this "meteorite" layer may have been terrestrial in origin, perhaps emplaced during the Flood by supercritical water or another means (Simon et. al., 2004). And if that iron layer was already in the ground, then the "meteorite" chunks found on the desert floor may just be terrestrial magnetite that was transformed due to the intense heat and pressure of a steam explosion. The 'meteorite' iron mineral "Widmanstätten pattern" can be formed at temperatures as low as 450C, and it has been observed in non-meteorite iron alloys such as carbon steel. One way to test this hypothesis is to drill additional holes progressively further from the crater and see

Figure 12. Barringer Craters and Nearby Volcanic Features

how far away from the crater this iron-rich layer persists – if it was a pre-existing deposit, then perhaps it extends a kilometer or more from the crater rim, whereas if it truly is from a meteor, then it should not extend nearly that far. Indeed, this terrestrial origin hypothesis for the source of the scattered iron was suggested by Fletcher in 1906 (Fletcher, 1906).

There is other evidence, not often discussed, that there were possible signs of volcanism associated with this crater. For one, Barringer discovered pumice in some of his boreholes – in some cases it was so light that it floated on the ground water in the holes (Hoyt, 1987). While it is argued that pumice can form from impacts, it is so commonly associated with volcanism that this seems more like an ad hoc rescuing device than a serious argument. Perhaps that's why Mallet, the geologist to whom Barringer sent the sample, said it has "the general character of siliceous sinter or geyserite from hot springs, and so seem to furnish some evidence of a kind, which I had supposed from your account to be entirely lacking, in support of Dr. Gilbert's steam explosion theory". Furthermore, one objection to the impact hypothesis was that there was never enough iron found to account for a meteorite large enough to create such a crater. A typical answer to this objection has been that most of the iron meteorite vaporized, and that's why it isn't found. However, if it vaporized, that would not eliminate the iron atoms, as the vapor must eventually condense, solidify, and fall to the surface of the ground in a fine powder of iron all around the crater and-or mixed in within the ejecta blanket, with enough volume to account for the entire size of the impactor. So this objection appears to still have merit.

The evidence in favor of each hypothesis can be summarized as follows:

(Table 1 – Barringer Crater Hypothesis Comparison)

So the Berringer Crater is not unambiguously an impact crater, but instead it bears many similarities to steam explosion craters which are fairly common in the Southwest United States and northern Mexico, and it has no distinguishing features that could not also be explained if it is in fact a steam explosion crater. Furthermore, there are several features of the site that are more consistent with a steam explosion than with an impact.

B. Lunar Crater Types That Require A Volcanic Origin

What about lunar craters – what evidence is there that they were formed via volcanic processes as opposed to impacts? Now that we have discussed the evidence for heat from accelerated nuclear decay throughout the solar system, and have considered the historical debate of craters having their origin from impacts or internal explosions, we can adequately address this question.

In addition to the massive volcanic eruptions that fill the "impact" basins on the near side of the Moon, as discussed above, quite a few smaller lunar craters have evidence of associated volcanism. In particular, the following three features show an association between many craters and volcanism, suggesting that, at the very least, craters with those characteristics were likely formed by explosive volcanic eruptions and not by impacts: 1) Irregular Mare Patches, 2) Lunar Rilles, and 3) Off-Center "Central" Peaks, some of which have summit pits.

Table 1. Barringer crater evidence comparison

Barringer Crater Observation	Impact Hypothesis	A.N.D. Steam Explosion Hypothesis
Crater size and shape	X	X
Shock metamorphism	X	X
Shatter Cones	X	X
Planar Deformation Features	X	X
Proximity to volcanoes		X
Relatively small quantity of iron		X
10m thick iron rich rock layer outside crater		X
Pumice in bore holes		X
Groundwater at 185m depth		X

1. Irregular Mare Patches

Irregular Mare Patches are areas that appear to be recent lava deposits, and they are found in and around the maria. These patches generally are found in small craters and generally appear like lumps that are largely devoid of craters themselves. Figure 13 contains several examples.

A paper in Nature Geoscience says, "The morphology of the features is also consistent with small basaltic eruptions that occurred significantly after the established cessation of the lunar mare basaltic volcanism" (Braden et. al., 2014). In the old-age uniformitarian paradigm, these basaltic eruptions, which they claim occurred roughly 100 million years ago (or over 3 billion years after the formation of the maria) are a mystery, since the Moon should have cooled and solidified long before that time. However in a Young-Earth paradigm, this fits the exponential decline of post-Flood volcanoes that we also see on Earth. Volcanic activity gradual tapered off as the remnant heat from the episode of accelerated radioactive decay near the surface of those worlds slowly dissipated over the last several thousand years (Austin, 1998). Furthermore, the association between irregular mare patches and the craters they are typically found within suggests a connection between the formation of those craters and their subsequent filling with lava. Figure 14 illustrates the abundance of these patches. If these craters containing recent lava flows were likely

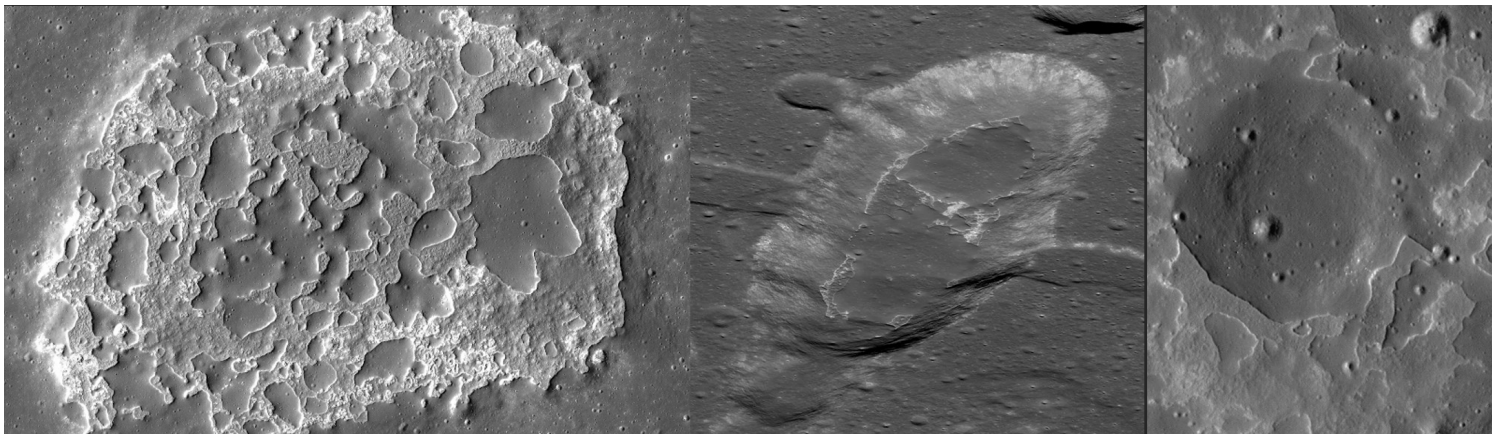

Figure 13. Irregular Lunar Mare Patches

formed volcanically, then perhaps other craters were as well.

2. Lunar Rilles

A lunar rille is a canyon on the moon that was likely carved by a flow of lava across the surface of the Moon. Note that these are not thermal expansion cracks like those discussed previously, but instead bear all the marks of being carved by a rapidly flowing fluid. Some rilles are very large, several kilometers across. While some rilles have been degraded since their formation, and their origin point is now unknown, many rilles clearly originate from craters. It appears as though the heat from a plume of rising magma first caused an explosion to form the crater, and then as it continued rising, it filled the newly formed crater and overtopped it, causing rapid draining of the newly filled crater as the overtopping lava quickly eroded the side of the new, unconsolidated crater wall. This rapid outflow of lava was able to then carve a large channel in the surface of the moon. Something very similar happened at the Taum Sauk pumped storage pond in Missouri. Once the water overtopped a low spot in the wall, the water drained catastrophically creating a channel where it

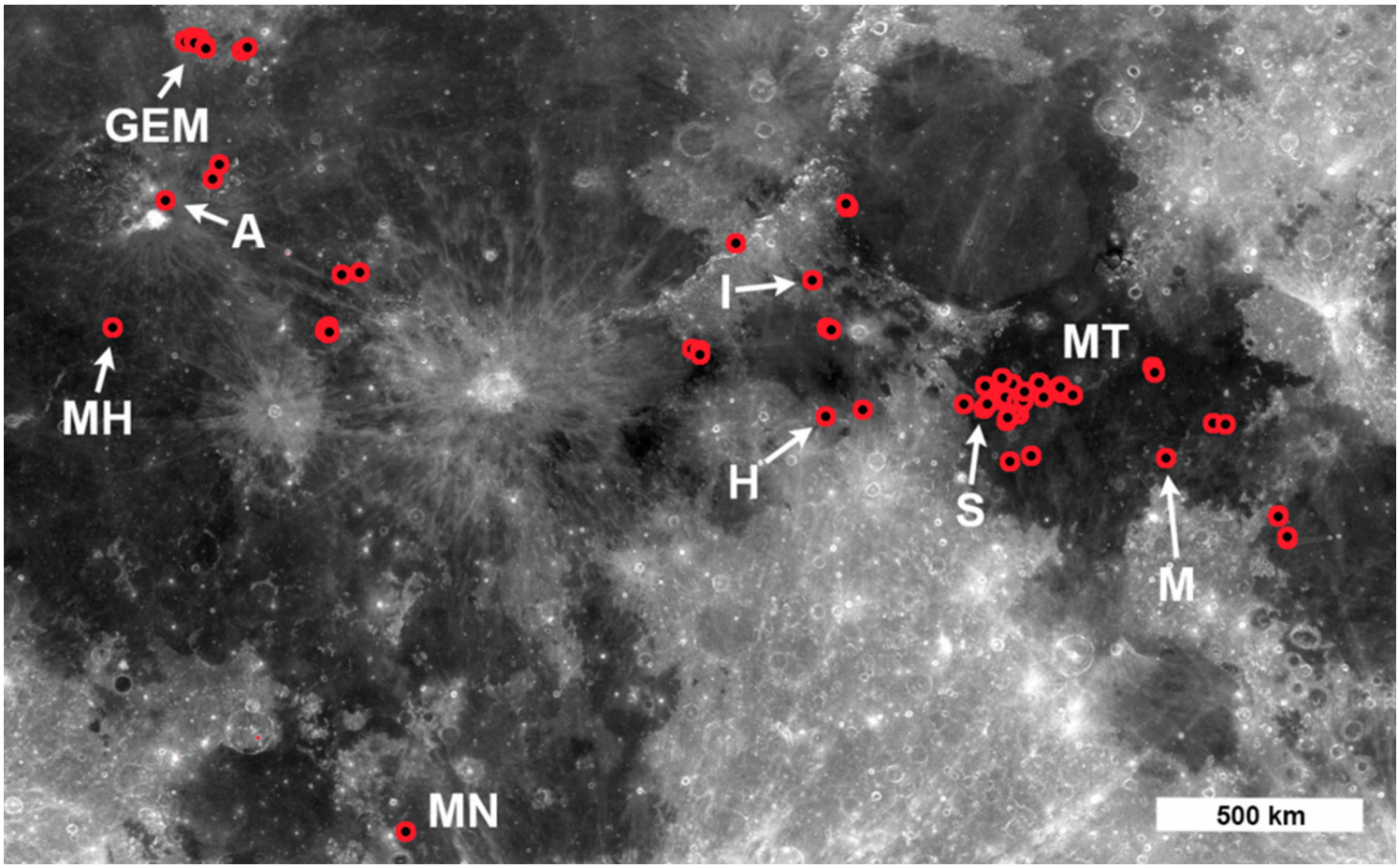

Figure 14. Map of Irregular Lunar Mare Patch Locations

flowed. (Figure 15) In response to this rille formation hypothesis, Jim Zimbelman of the Smithsonian Institution said, "I am quite sure that you are correct that the craters associated with rilles are somehow directly linked.…there is plenty of evidence in lunar soils of glass beads of different colors, with surface volatiles that suggest a pyroclastic eruption origin" (Zimbelman, 2014). (Figure 16) If these craters from which rilles originate were likely formed volcanically, then perhaps other craters were as well.

3. Off Center "Central" Peaks & Peaks With Summit Pits

While central peaks in craters have been used to argue for an impact formation of craters, when the peaks are not found in the center of the crater, or when the peaks themselves have summit pits, the more likely origin of those peaks is a volcanic one. A survey of 580 lunar central peaks was done in 1975 that discovered that about half of all central peaks are off center, and about a quarter of the central peaks investigated have summit pits – several of which "have what appear to be flows issuing from them" (Allen, 1975). This paper by Allen concludes that volcanism played a more important role in central peak formation than previously recognized. And if a volcano formed the central peak, then perhaps also a volcanic explosion formed the crater in the first place, followed by the eruption of lava shortly thereafter, just like we saw with the lunar rilles and the irregular mare patches. Indeed, we find several steam explosion craters on Earth with central peaks that appear to have formed in just this way, including the Zuni crater in western New Mexico and an unnamed crater in northern Chad at the coordinates 20.974144, 16.570422. Of course volcanic craters can also have central peaks such as Crater Lake in Oregon. So again, these lunar craters with off center central peaks and central peaks with summit pits strongly indicate that those craters were also formed volcanically.

Since it's clear that many smaller lunar craters must have a volcanic origin, and none of the craters on the moon (given what we know about them) *must* be impact craters, it makes sense to consider the hypothesis that the vast majority of lunar craters are volcanic in origin. It could be, however, that some of the more "recent" craters that have long debris trails emanating from them, such as Tycho crater, were formed from impacts after the pulse of accelerated decay produced most of the other craters and the surface of the moon had some time to cool. Perhaps in that case the impactor was ejected into an unstable orbit around the earth or moon by a prior mega volcanic explosion on the moon.

C. Mare Craters Likely Formed By Heat from Accelerated Nuclear Decay

Could even the large "impact" basins on the moon instead have been caused by massive explosions driven by heat from accelerated decay? The size of a crater is roughly proportional to the energy needed to form that crater, and for a crater the size of Mare Imbrium, at 1146 km across, approximately 10^{26} J of energy would be needed (Hughes, 2003). This is nearly an order of magnitude less than the total amount of energy that would have been released in accelerated radioactive decay just by the isotopes now located in the mare basalts that fill the crater, assumed to be an average of 1.3 km deep (Thomson et. al., 2009), which would have released approximately $9*10^{26}$ J. This amount of energy is sufficient not only to form the crater but also to heat and melt the mare basalts themselves. (Appendix C)

Further evidence that Imbrium and other "impact" basins were formed by rising magma causing massive explosions can be found in the detailed analysis of an unusual rock found on the moon. Although the rock has many indications that it is from the Moon, such as its iron content, lead isotope composition, and bulk geochemistry, its zircons and the presence of titanium within its quartz inclusions indicate that it was formed at a depth of more than 150 km below the lunar surface. (Bellucci et. al., 2019). This depth of formation is thought to be inconsistent with the impact formation hypothesis for the Imbrium "impact" basin. While the authors speculate that this rock may have a terrestrial origin, they note that it is plausible that this rock formed at the base of the lunar crust. Nevertheless, they fail to postulate any kind of mechanism for bringing such a deeply placed rock to the surface. The volcanic crater formation hypothesis proposed herein could explain how a rock from so deep within the

Figure 15 . Taum Sauk Pumped Hydro Catastrophic Drainage (Before and After)

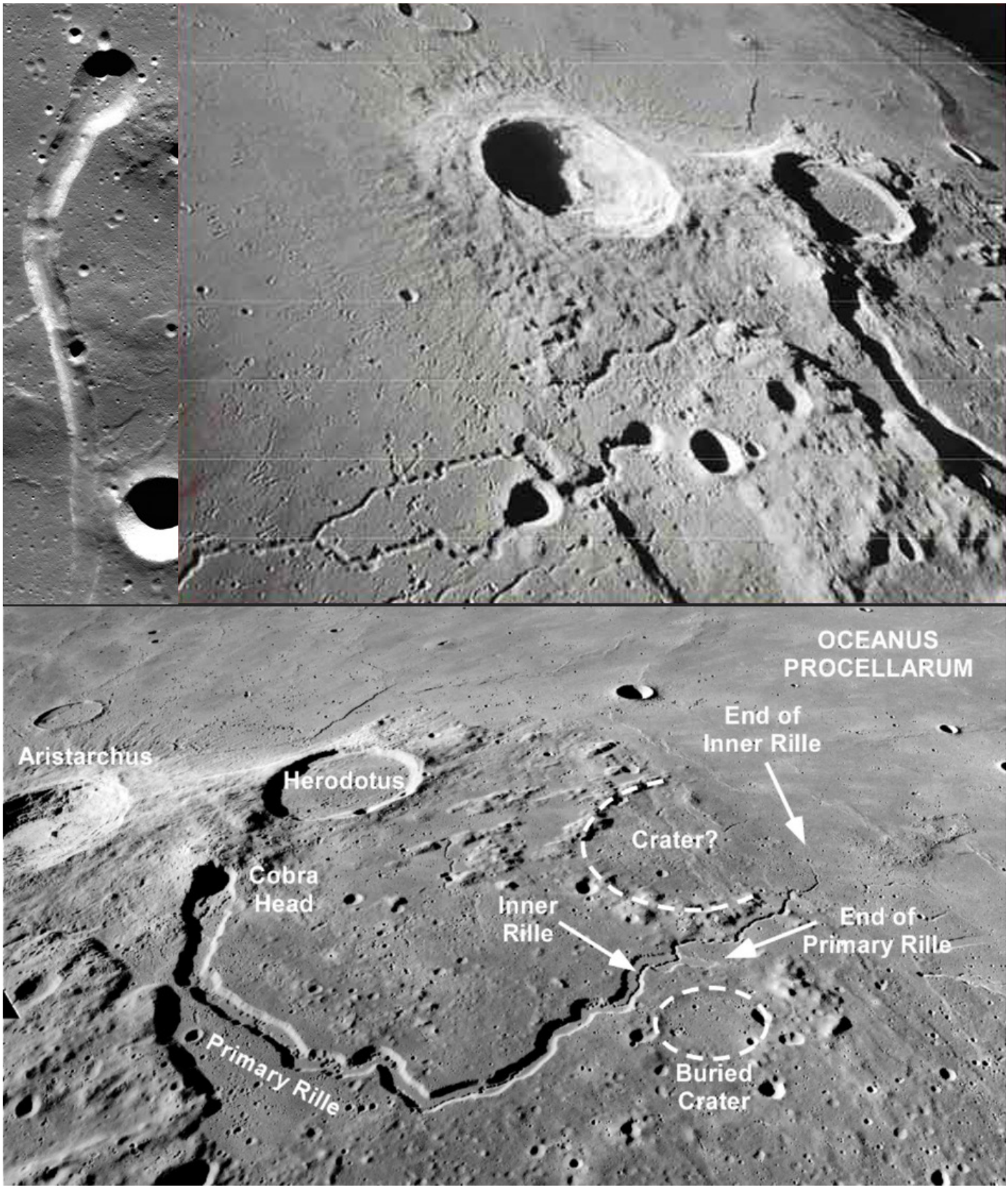

Figure 16. Lunar Rilles Originating from Craters

moon could be ejected onto its surface, similar to kimberlite pipe on Earth.

Finally, the existence of "ghost craters", smaller craters within the maria that are mostly filled with lava, can be best explained with this hypothesis. These ghost craters strongly suggest that there were many craters being formed between the event that caused the "impact basins" and their subsequent filling with lava (Faulkner, 1999). While it could indicate a high rate of bombardment by meteorites, it could also suggest that craters were still forming due to heat from accelerated decay between the time of the "impact" basin explosion and its subsequent filling with lava.

Thus, it is at least plausible that heat energy from accelerated radioactive decay could provide enough energy to form even the largest of the "impact" basins on the moon.

D. Possible Explosion Mechanisms

There seems to be a pattern of craters on the moon that are associated with lava flows. In each case, first there was an explosion forming a crater and then subsequently the newly formed crater was filled with lava to some extent. This is true in the cases of craters with irregular mare patches, craters with rilles, craters with volcanic central peaks, and "impact" basin craters. This patten hints at possible mechanisms for the generation of craters due to the heat of accelerated nuclear decay.

The basic cause of volcanic explosions is the right combination of heat, pressure, and a volatile substance that can very quickly change from a supercritical fluid or liquid to a gas. On Earth, for acknowledged maar craters, this substance is usually water. The pressure is due to the weight of the overlying rocks. So as this heated water makes its way toward the surface, at some point the pressure from the overlying rocks becomes just slightly less than the vapor pressure of the water. As a direct result of this, it flashes to steam almost instantaneously. The amount of hot fluid will determine the size of the explosion and subsequent crater.

If there is a large pocket of heated water, once the top portion of that pocket experiences an overburden pressure lower than its vapor pressure, that top part of the explodes. This removes the overburden for long enough for the entire pocket to experience a lower pressure, leading to the entire pocket exploding immediately. If there is a column of a hot volatile liquid, such as supercritical water, extending deep into the crust, then the explosive processes could well begin at the surface but continue down for quite a distance. Kimberlite pipes could be the result of exceptionally narrow and deep columns of supercritical water exploding in an instant.

On Earth there is clearly enough water for it to be the pressurized fluid that causes phreatic explosions. There was likely also enough water on Mars as well. It is less clear that Mercury or the Moon would have had enough subsurface water. If they were originally formed cool, then there would have been more potential for their interiors to house water in liquid or solid form, and it may have been more prevalent as mineral hydrates like gypsum. A recent reanalysis of samples returned on the Apollo missions have found more water than previously reported (Hui et. al., 2013). It also may be possible that some percentage of the oxides on asteroids and the Moon (e.g. CaO) were created as carbonates (e.g. $CaCO_3$) in which case the heat from the pulse of accelerated radioactive decay would have caused a chemical reaction releasing massive amounts of carbon dioxide. Indeed, carbonates have been found on dwarf planet Ceres (DeSanctis et. al., 2016). Deep enough under the surface, the carbon dioxide would have been a supercritical fluid, which could then have exploded powerfully as it approached the surface. Furthermore, given the extremely high heat production that would have occurred during accelerated radioactive decay, especially for minerals with the highest concentrations of radioactive isotopes, it is possible that some minerals like silica may have been heated, under pressure, to a temperature that exceeded their unpressurized boiling point. Perhaps the rocks themselves were the fluid that flashed to vapor in an instantaneous explosion. It is possible that all of these fluids played a role in crater formation during accelerated decay. We do know that some of the basalts returned from Mare Imbrium on the moon contain many gas bubbles that were still present when the rock solidified, so even if we don't know exactly which gas produced the bubbles, we do know that there was gas involved in the eruption. Figure 17 – Basalt rock returned from Mare Imbrium on the moon with many gas bubbles.

If accelerated nuclear decay produced craters on nearly all rocky planets and moons, why don't we see more large craters on Earth? On Earth, as well as perhaps on Venus, the whole mantle convection cycles that they experienced in part due to their large size and larger gravity field may have concentrated these explosive fluids at spreading zones, such as mid-ocean ridges on Earth, which would reduce their likelihood of causing massive explosions elsewhere. This may be part of the reason that we don't see the same number and size of craters on Earth as we do on the Moon. Another reason is that the Flood on Earth would have buried or eroded many of the craters that might have formed. And some people have even questioned whether some of the large craters we do see on Earth are impacts at all, and have proposed unusual types of volcanism for their formation (Wieland, 2006).

If this volcanic cratering hypothesis is correct, that heat from accelerated decay may have caused large pockets of superheated or supercritical fluids to form and then instantly flash to gas, then it seems possible that the majority of craters throughout the solar system may have actually been caused by this internal heat, and not by impacts. Perhaps the initial explosive fluid, hot molten temperature rock, supercritical water or carbon dioxide, was less viscous and less dense, so it would tend to rise more quickly. This hotter, lighter, less viscous material would create a diatreme which would then be followed later by cooler, more viscous and denser lava, which subsequently filled those newly formed craters. This pattern and its implied diatreme suggest a potential cause for the occasional crater found with concentric circles. It may be that an initially large explosion was followed by a smaller secondary explosion whose fluids travelled up the same diatreme at a later time. And again, this mechanism is consistent with the pattern mentioned earlier that seems to hold for craters with irregular mare patches, craters with rilles, craters with volcanic central peaks, and "impact" basin craters.

E. Crater Explosion Hypothesis Compared to Impact Hypothesis

From the standpoint of Biblical History and creation science, the crater explosion hypothesis seems more plausible than the impact

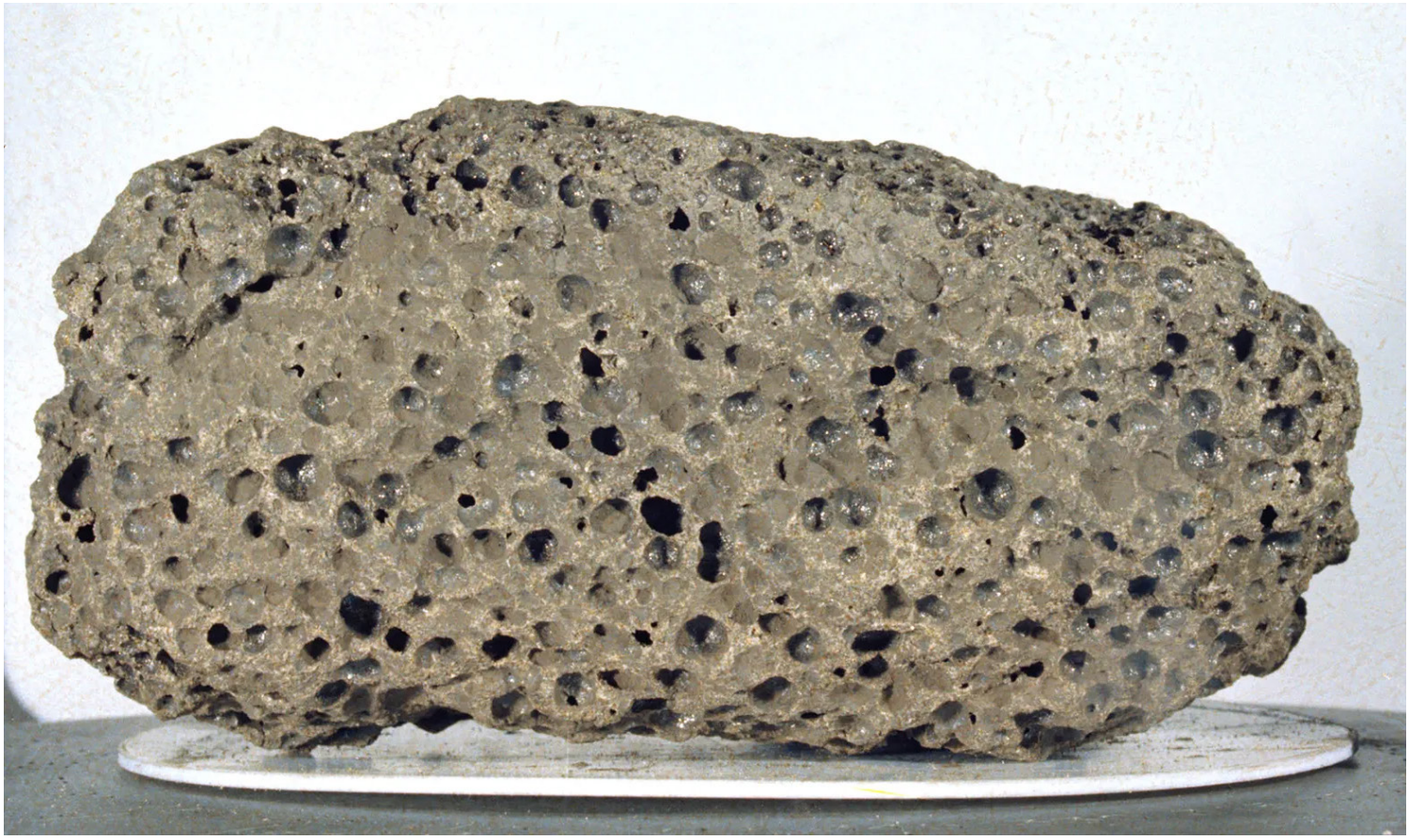

Figure 17. Lunar Basalt with Gas Bubbles

hypothesis for several reasons.

One of the primary objections to the impact hypothesis for creation scientists is that requires a huge number of large impactors to travel through the entire solar system so as to hit all of the rocky planets and moons from every direction in only a few thousand years, and to now be almost completely absent from the solar system. This seems implausible. (Spencer, 2013) There are a fairly large number of asteroids but almost none of them of any size seem to be on trajectories that would impact the planets and moons of the solar system.

Another weakness of the impact hypothesis is that it does a poor job of explaining lunar rilles, off center central peaks, central peaks with summit pits, irregular mare patches, massive thermal expansion cracks, and massive volcanoes. If all of these phenomena are best explained by heat from accelerated nuclear decay, then why also appeal to a massive swarm of impactors when they are not necessary to explain the evidence that we see? Indeed, other creationists have already proposed that craters are the result of accelerated radioactive decay – for instance, in 2000 Jim Hovis proposed that this internal heat caused the craters to form instead of impacts (Hovis, 2000).

IV. CONCLUSION

We have now examined a great deal of evidence which strongly suggests that the equivalent of approximately 4.5 billion years of accelerated decay occur throughout the solar system on or after Creation Day 4 in what appears to be one event that lasted for approximately one year. We also see that all of the heat from that decay was necessary to cause massive geological changes throughout the solar system, meaning that it was not miraculously removed. In addition to causing massive thermal expansion cracks, massive lava flows, the tectonic resurfacing of Venus, and other phenomena, this extreme pulse of heat energy likely also caused the vast majority of the craters seen on the rocky planets and moons of the solar system, contrary to the view that is currently popularly held among the secular scientific community. Perhaps those early creation scientists were right about the volcanic origin of craters, just as they were right about the global Flood.

Further study could be done on Earth by searching a variety of steam explosion craters for 'impact signatures' to see whether or not they truly are impact signatures. Also, more drilling could theoretically be done around the Berringer Crater to better characterize the layer of iron-rich rock was previously found in a borehole – perhaps by looking outside the crater a commercially useful quantity of iron could finally be found and mined.

REFERENCES

Braden, S., J. D. Stopar, M. S. Robinson, S. J. Lawrence, C.H van der Boghert, H. Hiesinger. 2014. Evidence for Basaltic Volcanism on the Moon Within the Past 100 Million Years. *Nature Geoscience*, 7(11):787-791. DOI: 10.1038/ngeo2252

Carter, R. 2012. Ancient Coral Growth Layers. *Journal of Creation*, 26(3):50-53.

Chu, J. 2014. Solving the Mystery of the "Man in the Moon", MIT News - Earth, Atmospheric and Planetary Sciences. Retrieved May 23, 2023, from: https://eapsweb.mit.edu/news/2014/solving-mystery-man-moon.

Clarey, T. 2017. Do the Data Support a Large Meteorite Impact at Chicxulub? *Answers Research Journal*, 10:71–88.

DeSanctis, M. C., A. Raponi, E. Ammannito, M. Ciarniello, M. J. Toplis, H. Y. McSween, J. C. Castillo-Rogez, B. L. Ehlmann, F. G. Carrozzo, S. Marchi, F. Tosi, F. Zambon, F. Capaccioni, M. T. Capria, S. Fonte, M. Formisano, A. Frigeri, M. Giardino, A. Longobardo, G. Magni, E. Palomba, L. A. McFadden, C. M. Pieters, R. Jaumann, P. Schenk, R. Mugnuolo, C. A. Raymond, C. T. Russell. 2016. Bright Carbonate Deposits as Evidence of Aqueous Alteration on (1) Ceres. *Nature*, 536(7614):54-57.

Faulkner, D. 1999. A Biblically-Based Cratering Theory. *Journal of Creation*, 13(1):100-104.

Fletcher, L. 1906. A Search for a Buried Meteorite. *Nature*, 74:490-492.

Grieve, R. A., M. Pilkington. 1996. The Signature of Terrestrial Impacts. *Journal of Australian Geology & Geophysics*, 16(4):399-420.

Harada, Y., , S. Goossens, K. Matsumoto, J. Yan, J. Ping, H. Noda, J. Haruyama. 2014. Strong Tidal Heating in an Ultralow-Viscosity Zone at the Core-Mantle Boundary of the Moon. *Nature Geoscience*, 7(8):569-572. DOI: 10.1038/ngeo2211

Hooke, R. 1665. *Micrographia*. London: J. Martyn and J. Allestry.

Hovis, J. 2000. Biblically-Based Cratering Theory. *Journal of Creation*. 14(3):74-75.

Hoyt, W. G. 1987. *Coon Mountain Controversies: Meteor Crater and the Development of Impact Theory*. Tucson: The University of Arizona Press.

Huffman, A. R., W. U. Reimold. 1996. Experimental Constraints on Shock-Induced Microstructures in Naturally Deformed Silicates. *Tectonophysics*, 256(1):165-217. DOI: 10.1016/0040-1951(95)00162-X

Hughes, D. 2003. The Approximate Ratios Between the Diameters of Terrestrial Impact Craters and the Causative Incident Asteroids. *Monthly Notices of the Royal Astronomical Society*, 338(4):999-1003. DOI: 10.1046/j.1365-8711.2003.06157.x

Hui, H., A. Peslier, Y. Zhang, C. R. Neal. 2013. Water in Lunar Anorthosites and Evidence for a Wet Early Moon. *Nature Geoscience*, 6(3):177-180. DOI:10.1038/NGEO1735

Humphreys, D. R. 2014. Magnetized Moon Rocks Shed light on Precambrian Mystery. *Journal of Creation*, 28(3):51-60.

Hynek, B., R. J. Phillips, R. E. Arvidson. 2003. Explosive Volcanism in the Tharsis Region: Global Evidence in the Martian Geologic Record. *Journal of Geophysical Research*, 108(9):15-1 to 15-16. DOI:10.1029/2003JE002062

King, D. A. 2017. *Guidebook to the Geology of Barringer Meteorite Crater, Arizona* (2nd Edition). Lunar and Planetary Institute.

Lyubestkaya, T., et. al.. 2009. Effect of Metamorphic Reactions on Thermal Evolution in Collisional Orogens. *Journal of Metamorphic Geology*, 27(8):579-600. DOI:10.1111/j.1525-1314.2009.00847.x

Nimmo, F., Tanaka, K. 2005. Early Crustal Evolution of Mars. *Annual Review of Earth Planetary Science*, 33(1):133-161. DOI:10.1146/annurev.earth.33.092203.122637

O'Neill, I. 2014. 'Man in the Moon' Created by Mega Volcano, Discovery News. Retrieved May 23, 2023 from: https://web.archive.org/web/20141003035505/http://news.discovery.com/space/the-man-in-the-moon-was-created-by-mega-volcano-141001.htm

Phillips, R. J., M. T. Zuber, S. C. Solomon, M. P. Golombek, B. M. Jakosky, W. B. Banerdt, D. E. Smith, R. M. E. Williams, B. M. Hynek, O. Aharonson, S. A. Hauck. 2001. Ancient Geodynamics and Global-Scale Hydrology on Mars. *Science*, 291(5513):2587-2591. DOI: 10.1126/science.1058701

Samec, R. 2000. The Age of Jovian Planets. *Journal of Creation*, 14(1):3-4.

Samec, R. 2014. Has Mars Undergone One or More RATE Episodes? *Journal of Creation*, 28(1):68-76.

Shoemaker, E. 1962. Interpretation of Lunar Craters. In Z. Kopal, *Physics and Astronomy of the Moon*. New York and London: Academic Press, pp. 283-359.

Simon, A., T. Pettke, P. A. Candela, P. M. Piccoli, C. A. Heinrich. 2004. Magnetite Solubility and Iron Transport in Magmatic-Hydrothermal Environment. *Geochimica et Cosmochimica Acta*, 68(23):4905-4914. DOI: 10.1016/j.gca.2004.05.033

Snelling, A. A. 2012. Solving the Mystery of the Missing Bullets - Part 3. *Answers Magazine*. 7(4):70-73.

Spencer, Wayne. 2013. Impacts and Noah's Flood—How Many And Other Issues. *Journal of Creation*, 27(1):85-89.

Spudis, P. 2010. A Founding Father of Lunar Science. *Air & Space (Smithsonian)*.

Steigerwald, B., N. Jones. NASA Press Release: Shrinking Moon May Be Generating Moonquakes. Release 19-06. May 13, 2019. (https://www.nasa.gov/press-release/goddard/2019/moonquakes).

Stenberg, D. B. 2012. A New Magnetic Field Theory and Flood Model. *Journal of Creation*, 26(2):57-69.

Strom, R., G. G. Schaber, D. D. Dawson. 1994. The Global Resurfacing of Venus. *Journal of Geophysical Research*, 99(E5):10899-10926. DOI: 10.1029/94JE00388

Taylor, F., H. Svedhem, J. W. Head. 2018. Venus: The Atmosphere, Climate, Surface, Interior and Near-Space Environment of an Earth-Like Planet. *Space Science Reviews*, 214(1):35. DOI:10.1007/s11214-018-0467-8

Thomson, B. J., E. B. Grosfils, D. B. J. Bussey, P. D. Spudis. 2009. A New Technique for Estimating the Thickness of Mare Basalts in Imbrium Basin. *Geophysical Research Letters*, L12201, 36(12):1-5. DOI:10.1029/2009GL037600

Vardiman, L., A. A. Snelling, E. F. Chaffin (editors). 2005. *Radioisotopes and the Age of the Earth - Results of a Young-Earth Creationist Research Initiative*. El Cajon: Institute for Creation Research.

Wieland, Carl. 2006. Immense Impacts or Big Belches? *Creation*, 28(2):24-27.

Wise, K. 2018. Fossil Grove and Other Paleozoic Forests as Allochthonous Flood Deposits. *Answers Research Journal*, 11:247-266.

Zuber, M. 2018. Oceans on Mars Formed Early. *Nature*, 555(7698):590-591. DOI: 10.1038/d41586-018-03415-x

Zuber, M., J. C. Andrews-Hanna, J. Besserer, J. W. Head III, C. J. A. Howett, W. S. Kiefer, P. J. Lucey, P. J. McGovern, H. J. Melosh, G. A. Neumann, R. J. Phillips, P. M. Schenk, D. E. Smith, S. C. Solomon. 2014. Structure and Evolution of the Lunar Procellarum Region as Revealed by GRAIL Gravity data. *Nature*, 514(7520):68-71. DOI: 10.1038/nature13697

THE AUTHOR

Don Stenberg, Jr. earned his BS in Mechanical Engineering at Dordt College in 2004 and his M.Div. at Cornerstone Seminary in 2012. He has been closely following developments in creation science for over 20 years. He currently lives in Missouri with his wife and eight children, and works from home as an Information Services Manager.

APPENDIX A – THERMAL CALCULATIONS OF THE MOON

Sheet 1 Explanatory Notes — Accelerated Decay

Here we calculate the energy available on the Moon from accelerated nuclear decay equivalent to that which would emerge over the

conventionally dated age of the Earth. We consider the major radionuclides to be **Uranium-235**, **Uranium-238**, **Thorium-232** and **Potassium-40** with principal decay modes known to be **Alpha** for the heavy isotopes and **Beta** for potassium. In the absence of data to the contrary, the relative abundances of these isotopes have been assumed to be the same as those on Earth, with data on Uranium being available for the bulk Moon (**2**) and Thorium concentration data for its surface (**12,13**). It is also assumed that the current crust/mantle ratios for the Moon and Earth are the same. These can be combined to give the bulk result shown in Cell **F29** and found to be between that of Earth and the revised estimate from Drake et al (**2**). References for input data are highlighted in yellow, with cited sources in the **References** table. If data is taken from another cell in the same sheet, the cell reference is shown, highlighted in cyan. If it is from another sheet, the sheet number appears before the cell reference. Key result fields are highlighted to the right in magenta.

References

Sheet 2 Explanatory Notes — Gravitational Energy

No.	Source
1	https://en.wikipedia.org/wiki/Moon
2	Drake M J, Lowe J P, Righter K, Zuber M T & Clark P E, **Uranium in the Lunar Crust: Implications for Lunar Origin and Evolution**, Proc. 61st Annual Meteoritical Society Meeting, 5174.pdf (1998)
3	https://en.wikipedia.org/wiki/Internal_structure_of_the_Moon
4	https://en.wikipedia.org/wiki/Anorthite
5	https://en.wikipedia.org/wiki/Iron
6	https://en.wikipedia.org/wiki/Uranium-235#Natural_decay_chain
7	https://arxiv.org/abs/hep-ph/0409152v1
8	https://en.wikipedia.org/wiki/Electron
9	https://en.wikipedia.org/wiki/Avogadro_constant
10	https://en.wikipedia.org/wiki/Abundances_of_the_elements_(data_page)
11	https://en.wikipedia.org/wiki/Potassium-40
12	https://en.wikipedia.org/wiki/KREEP#/media/File:Lunar_Thorium_concentrations.jpg
13	Metzger A E, Haines E L, Parker R E & Radocinski R G, **Thorium Concentrations in the Lunar Crust: Part 1 - Regional Values and Crustal Content**, Proc. 8th Lunar Scientific Conference, 949-999 (1977)
14	https://en.wikipedia.org/wiki/Age_of_the_Earth

Table 1 - Crust Mantle and Core Masses			
Parameter	**Amount**	**Units**	**Ref**
$R_{Overall}$	1.74E+06	m	1
t_{Crust}	6.40E+04	m	2
$R_{Upper\ Mantle} = R_O - t_C$	1.67E+06	m	
$R_{Outer\ Core}$	3.30E+05	m	3
$R_{Inner\ Core}$	2.40E+05	m	3
$V_{Overall} = 4\pi R_O^3/3$	2.20E+19	m^3	
$V_{Crust} = 4\pi(R_O - t_C/2)^2 t_C$	2.34E+18	m^3	
$V_{Mantle} = 4\pi(R_{UM}^3 - R_{OC}^3)/3$	1.95E+19	m^3	
$V_{Outer\ Core} = 4\pi(R_{OC}^3 - R_{IC}^3)/3$	9.26E+16	m^3	
$V_{Inner\ Core} = 4\pi R_{IC}^3/3$	5.79E+16	m^3	
$\rho_{Average}$	3346	kg/m^3	3
ρ_{Crust}	2735	kg/m^3	3,4
$\rho_{Mantle} = M_M/V_M$	3399	kg/m^3	B11,21
$\rho_{Outer\ Core}$	5000	kg/m^3	3
$\rho_{Inner\ Core}$	7874	kg/m^3	3,5
$M_{Overall} = \rho_A V_O$	7.35E+22	kg	
$M_{Crust\ Moon} = \rho_C V_C$	6.40E+21	kg	Result
$M_{Mantle\ Moon} = M_O - M_C - M_{OC} - M_{IC}$	6.62E+22	kg	Result
$M_{Outer\ Core} = \rho_{OC} V_{OC}$	4.63E+20	kg	
$M_{Inner\ Core} = \rho_{IC} V_{IC}$	4.56E+20	kg	

Table 2 - Decay Specific Energy Units Conversion			
Parameter	**Amount**	**Units**	**Ref**
$E_{Specific}(^{235}U)$	4.68E+07	eV/atom	6
$E_{Specific}(^{238}U)$	5.17E+07	eV/atom	7
$E_{Specific}(^{232}Th)$	4.27E+07	eV/atom	7
$E_{Specific}(^{40}K)$	1.32E+06	eV/atom	7
q(electron)	1.60E-19	J/eV	8
$N_{Avogadro}$	6.02E+23	atoms/mol	9
$A(^{235}U)$	2.35E-01	kg/mol	
$A(^{238}U)$	2.38E-01	kg/mol	
$A(^{232}Th)$	2.32E-01	kg/mol	
$A(^{40}K)$	4.00E-02	kg/mol	
$E_{Specific}(^{235}U) = E_S(^{235}U)qN_A/A(^{235}U)$	1.92E+13	J/kg	
$E_{Specific}(^{238}U) = E_S(^{238}U)qN_A/A(^{238}U)$	2.10E+13	J/kg	
$E_{Specific}(^{232}Th) = E_S(^{232}Th)qN_A/A(^{232}Th)$	1.78E+13	J/kg	
$E_{Specific}(^{40}K) = E_S(^{40}K)qN_A/A(^{40}K)$	3.18E+12	J/kg	

Table 3 - Current Radioisotope Inventories			
Parameter	**Amount**	**Units**	**Ref**
$[U]_{Crust\ Earth}$	2.70E-06	kg/kg	10
$[^{232}Th]_{Crust\ Earth}$	9.60E-06	kg/kg	10
$[^{40}K]_{Crust\ Earth}$	2.51E-06	kg/kg	10,11
$[U]_{Crust\ Moon} = [^{232}Th]_{CM}[U]_{CE}/[^{232}Th]_{CE}$	1.97E-07	kg/kg	F8
$[^{232}Th]_{Crust\ Moon}$	7.00E-07	kg/kg	12,13
$[^{40}K]_{Crust\ Moon} = [^{232}Th]_{CM}[^{40}K]_{CE}/[^{232}Th]_{CE}$	1.83E-07	kg/kg	F8
$[U]_{Mantle\ Earth}$	3.30E-08	kg/kg	7
$[^{232}Th]_{Mantle\ Earth}$	1.32E-07	kg/kg	7
$[^{40}K]_{Mantle\ Earth}$	3.96E-08	kg/kg	7
$[U]_{Mantle\ Moon} = [U]_{CM}[U]_{ME}/[U]_{CE}$	2.41E-09	kg/kg	F7
$[^{232}Th]_{Mantle\ Moon} = [U]_{MM}[^{232}Th]_{ME}/U_{ME}$	9.63E-09	kg/kg	F11
$[^{40}K]_{Mantle\ Moon} = [U]_{MM}[K]_{ME}/U_{ME}$	2.89E-09	kg/kg	F12
$M_{Crust\ Moon}(U) = M_{CM}[U]_{CM}$	1.26E+15	kg	B20,F7
$M_{Crust\ Moon}(^{232}Th) = M_{CM}[^{232}Th]_{CM}$	4.48E+15	kg	B20,F8
$M_{Crust\ Moon}(^{40}K) = M_C[^{40}K]_C$	1.17E+15	kg	B20,F9
$M_{Mantle\ Moon}(U) = M_M[U]_M$	1.59E+14	kg	B21,F13
$M_{Mantle\ Moon}(^{232}Th) = M_M[^{232}Th]_M$	6.37E+14	kg	B21,F14
$M_{Mantle\ Moon}(^{40}K) = M_M[^{40}K]_M$	1.91E+14	kg	B21,F15
$M_{Total}(U) = M_C(U) + M_M(U)$	1.42E+15	kg	
$M_{Total}(^{232}Th) = M_C(^{232}Th) + M_M(^{232}Th)$	5.11E+15	kg	
$M_{Total}(^{40}K) = M_C(^{40}K) + M_M(^{40}K)$	1.36E+15	kg	
$[^{235}U]/[U]$	0.72%	kg/kg	6
$M_{Total}(^{235}U) = M_T(U)[^{235}U]/[U]$	1.02E+13	kg	

Table 3 - Current Radioisotope Inventories			
Parameter	**Amount**	**Units**	**Ref**
$[^{238}U]/[U]$	99.27%	kg/kg	
$M_{Total}(^{238}U) = M_T(U)[^{238}U]/[U]$	1.41E+15	kg	
$M_{Total}(U)/M_{Lunar\ Total}$	1.93E-08	kg/kg	2

Table 4 - Accelerated Decay Energy			
Parameter	**Amount**	**Units**	**Ref**
Uniformitarian Decay Time (t_{Total})	4.54E+09	year	13
$t_{Half}(^{235}U)$	7.04E+08	year	6
$t_{Half}(^{238}U)$	4.47E+09	year	7
$t_{Half}(^{232}Th)$	1.40E+10	year	7
$t_{Half}(^{40}K)$	1.28E+09	year	7
$t_{Total}/t_{Half}(^{235}U)$	6.45	year/year	
$t_{Total}/t_{Half}(^{238}U)$	1.02	year/year	
$t_{Total}/t_{Half}(^{232}Th)$	0.32	year/year	
$t_{Total}/t_{Half}(^{40}K)$	3.55	year/year	
$2^{tT/tHU235} = 2\text{^}[t_{Total}/t_{Half}(^{235}U)]$	87.47	kg/kg	
$2^{tT/tHU238} = 2\text{^}[t_{Total}/t_{Half}(^{238}U)]$	2.02	kg/kg	
$2^{tT/tHTh232} = 2\text{^}[t_{Total}/t_{Half}(^{232}Th)]$	1.25	kg/kg	
$2^{tT/tHK40} = 2\text{^}[t_{Total}/t_{Half}(^{40}K)]$	11.69	kg/kg	
$M_{Current}(^{235}U)$	1.02E+13	kg	F28
$M_{Current}(^{238}U)$	1.41E+15	kg	F30
$M_{Current}(^{232}Th)$	5.11E+15	kg	F25
$M_{Current}(^{40}K)$	1.36E+15	kg	F26
$M_{Initial}(^{235}U) = 2^{tT/tHU235}M_C(^{235}U)$	8.93E+14	kg	
$M_{Initial}(^{238}U) = 2^{tT/tU238}M_C(^{238}U)$	2.85E+15	kg	
$M_{Initial}(^{232}Th) = 2^{tT/tHTh232}M_C(^{232}Th)$	6.40E+15	kg	
$M_{Initial}(^{40}K) = 2^{tT/tHK40}M_C(^{40}K)$	1.59E+16	kg	
$\Delta M(^{235}U) = M_I(^{235}U) - M_C(^{235}U)$	8.83E+14	kg	
$\Delta M(^{238}U) = M_I(^{238}U) - M_C(^{238}U)$	1.44E+15	kg	

Table 4 - Accelerated Decay Energy			
Parameter	**Amount**	**Units**	**Ref**
$\Delta M(^{232}Th) = M_I(^{232}Th) - M_C(^{232}Th)$	1.29E+15	kg	
$\Delta M(^{40}K) = M_I(^{40}K) - M_C(^{40}K)$	1.45E+16	kg	
$E_{Specific}(^{235}U)$	1.92E+13	J/kg	B26
$E_{Specific}(^{238}U)$	2.10E+13	J/kg	B27
$E_{Specific}(^{232}Th)$	1.78E+13	J/kg	B28
$E_{Specific}(^{40}K)$	3.18E+12	J/kg	B29
$E_{Total}(^{235}U) = E_S(^{235}U)\Delta M(^{235}U)$	1.70E+28	J	
$E_{Total}(^{238}U) = E_S(^{238}U)\Delta M(^{238}U)$	3.02E+28	J	
$E_{Total}(^{232}Th) = E_S(^{232}Th)\Delta M(^{232}Th)$	2.29E+28	J	
$E_{Total}(^{40}K) = E_S(^{40}K)\Delta M(^{40}K)$	4.63E+28	J	
$E_{Grand\ Total\ Decay}$	1.16E+29	J	Result

Here we calculate the gravitational potential difference that would be met by the decay-heat-induced expansion of the Moon, which is currently divided into the layers with the labels **Inner Core**, **Outer Core**, **Lunar Mantle** and **Lunar Crust**. As it is assumed to be initially cool and solid, with a homogeneous mantle, the initial Moon is partitioned simply into **Core Initial** and **Mantle Initial**, with trial values for initial radii. Volumes emerging from these trials are then fed into **Sheet 3** for a calculation of initial temperature. The trial values are then adjusted to yield an initial temperature of order 300 K (27°C). There are, listed and derived above, formulae used to calculate potential energy for spherically symmetric bodies. References for input data are highlighted in yellow, with cited sources in the **References** table. If data is taken from another cell in the same sheet, the cell reference is shown, highlighted in cyan. If it is from another sheet, the sheet number appears before the cell reference. Along with key results, a magenta highlight indicates a trial input, such as initial surface and core radii, that are designed to produce the initially ambient temperature before thermal expansion, details of which appear in **Sheet 3**.

References

No.	Source
1	https://en.wikipedia.org/wiki/Gravitational_constant
2	https://en.wikipedia.org/wiki/Inner_core
3	https://en.wikipedia.org/wiki/Outer_core
4	https://en.wikipedia.org/wiki/Mantle_(geology)
5	Anderson D L, **Theory of the Earth**, Boston: Blackwell Scientific Publications (1989) http://resolver.caltech.edu/CaltechBOOK:1989.001 (see image below)
6	https://en.wikipedia.org/wiki/Earth_mass

Expansion Energy Formulae
Initial Conditions
$dU_{Core\ Initial} = -GMdM/R = -GM4\pi\rho R^2dR/R = -GM4\pi\rho RdR = -G(4\pi)^2\rho^2R^4dR/3$
$U_{Core\ Initial} = -G(4\pi)^2\rho_{CI}^2R_{CI}^5/15 = 3GM_{CI}^2/(5R_{CI})$
$dU_{Mantle\ Initial} = -GMdM/R = -G[M_{CI} + \rho_{MI}(4\pi R^3/3 - V_{CI})]\rho_{MI}4\pi RdR$
$U_{Mantle\ Initial} = -G[2\pi\rho_{MI}(M_{CI} - \rho_{MI}V_{CI})(R_{MI}^2 - R_{CI}^2) + 16\pi^2\rho_{MI}^2(R_{MI}^5 - R_{CI}^5)/15]$
$U_{Mantle\ Initial} = -G\rho_{MI}[2\pi(M_{CI} - \rho_{MI}V_{CI})(R_{MI}^2 - R_{CI}^2) + 16\pi^2\rho_{MI}(R_{MI}^5 - R_{CI}^5)/15]$
Current Conditions
$U_{Inner\ Core} = -3GM_{IC}^2/(5R_{IC})$
$U_{Outer\ Core} = -G[2\pi\rho_{OC}(M_{IC} - \rho_{OC}V_{IC})(R_{OC}^2 - R_{IC}^2) + 16\pi^2\rho_{OC}^2(R_{OC}^5 - R_{IC}^5)/15]$
$U_{Lunar\ Mantle} = -G[2\pi\rho_{LM}(M_{IC+OC} - \rho_{LM}V_{IC+OC})(R_{LM}^2 - R_{OC}^2) + 16\pi^2\rho_{LM}^2(R_{LM}^5 - R_{OC}^5)/15]$
$U_{Lunar\ Crust} = -G[2\pi\rho_{LC}(M_{IC+OC+LM} - \rho_{LC}V_{IC+OC+LM})(R_{LC}^2 - R_{LM}^2) + 16\pi^2\rho_{LC}^2(R_{LC}^5 - R_{LM}^5)/15]$
InTerms of Mass (Simple Core-Mantle System)
$U_{Mantle} = -G\rho_M[2\pi(M_C - \rho_MV_C)(R_M^2 - R_C^2) + 16\pi^2\rho_M(R_M^5 - R_C^5)/15]$
$U_{Mantle} = -GM_M[2\pi(M_C - \rho_MV_C)(R_M^2 - R_C^2) + 16\pi^2\rho_M(R_M^5 - R_C^5)/15]/[4\pi(R_M^3 - R_C^3)/3]$
$U_{Mantle} = -GM_M[(M_C - \rho_MV_C)(R_M^2 - R_C^2) + 8\pi\rho_M(R_M^5 - R_C^5)/15]/[2(R_M^3 - R_C^3)/3]$
$U_{Mantle} = -3GM_M[(M_C(R_M^2 - R_C^2) + \rho_M(4\pi R_C^3/3)(R_C^2 - R_M^2) + 8\pi\rho_M(R_M^5 - R_C^5)/15]/[2(R_M^3 - R_C^3)]$
$U_{Mantle} = -3GM_M[(M_C(R_M^2 - R_C^2) + (4\pi\rho_M/3)\{R_C^3(R_C^2 - R_M^2) + 2(R_M^5 - R_C^5)/5\}]/[2(R_M^3 - R_C^3)]$
$U_{Mantle} = -3GM_M[(M_C(R_M^2 - R_C^2) + M_M\{R_C^3(R_C^2 - R_M^2) + 2(R_M^5 - R_C^5)/5\}/(R_M^3 - R_C^3)]/[2(R_M^3 - R_C^3)]$
$U_{Mantle} = -3GM_M[(M_C(R_M^2 - R_C^2) + (M_M/5)(5R_C^5 - 5R_C^3R_M^2 + 2R_M^5 - 2R_C^5)/(R_M^3 - R_C^3)]/[2(R_M^3 - R_C^3)]$
$U_{Mantle} = -(3GM_M/2)\{(M_C(R_M^2 - R_C^2) + (M_M/5)(3R_C^5 - 5R_C^3R_M^2 + 2R_M^5)/(R_M^3 - R_C^3)\}/(R_M^3 - R_C^3)$

Table 1 - Current Potential Energy			
Parameter	**Amount**	**Units**	**Ref**
G	6.67E-11	$m^3kg^{-1}s^{-2}$	**1**
$R_{Inner\ Core}$	2.40E+05	m	**1.B8**
$R_{Outer\ Core}$	3.30E+05	m	**1.B7**
$R_{Lunar\ Mantle}$	1.67E+06	m	**1.B6**
$R_{Moon\ Current}$	1.74E+06	m	**1.B4**
$\rho_{Inner\ Core}$	7874	kg/m^3	**1.B18**
$\rho_{Outer\ Core}$	5000	kg/m^3	**1.B17**
$\rho_{Lunar\ Mantle}$	3399	kg/m^3	**1.B16**
$\rho_{Lunar\ Crust}$	2735	kg/m^3	**1.B15**
$V_{Inner\ Core}$	5.79E+16	m^3	**1.B13**
$V_{Outer\ Core}$	9.26E+16	m^3	**1.B12**
$V_{Lunar\ Mantle}$	1.95E+19	m^3	**1.B11**
$V_{Lunar\ Crust}$	2.34E+18	m^3	**1.B10**
$M_{Inner\ Core}$	4.56E+20	kg	**1.B23**
$M_{Outer\ Core}$	4.63E+20	kg	**1.B22**
$M_{Lunar\ Mantle}$	6.62E+22	kg	**1.B21**
$M_{Lunar\ Crust}$	6.40E+21	kg	**1.B20**
$U_{Inner\ Core} = -3GM_{IC}^2/(5R_{IC})$	-3.47E+25	J	
$M_{IC} - \rho_{OC}V_{IC}$	1.66E+20	kg	
$R_{OC}^2 - R_{IC}^2$	5.13E+10	m^2	
$R_{OC}^5 - R_{IC}^5$	3.12E+27	m^5	
$U_{Outer\ Core}$	-7.27E+25	J	**M20**
$M_{IC+OC} - \rho_{LM}V_{IC+OC}$	4.07E+20	kg	

Table 1 - Current Potential Energy			
Parameter	Amount	Units	Ref
$R_{LM}^2 - R_{OC}^2$	2.69E+12	m^2	
$R_{LM}^5 - R_{OC}^5$	1.31E+31	m^5	
$U_{Lunar\ Mantle}$	-1.08E+29	J	M21
$M_{IC+OC+LM} - \rho_{LC} V_{IC+OC+LM}$	1.34E+22	kg	
$R_{MC}^2 - R_{LM}^2$	2.18E+11	m^2	
$R_{MC}^5 - R_{LM}^5$	2.71E+30	m^5	
$U_{Lunar\ Crust}$	-1.76E+28	J	M22
$U_{Moon\ Current} = U_{IC} + U_{OC} + U_{LM} + U_{LC}$	-1.26E+29	J	Result

Table 2 - Initial Potential Energy			
Parameter	Amount	Units	Ref
G	6.67E-11	$m^3kg^{-1}s^{-2}$	B4
$R_{Core\ Initial}$	3.28E+05	m	Trial
$R_{Moon\ Initial}$	1.70E+06	m	Trial
$\rho_{Core\ Initial} = M_{CI}/V_{CI}$	6205	kg/m^3	
$\rho_{Mantle\ Initial} = M_{MI}/V_{MI}$	3535	kg/m^3	
$V_{Core\ Initial} = 4\pi R_{CI}^{\ 3}/3$	1.48E+17	m^3	
$V_{Mantle\ Initial} = 4\pi(R_{MI}^{\ 3} - R_{CI}^{\ 3})/3$	2.05E+19	m^3	
$V_{Moon\ Initial} = V_{CI} + V_{MI}$	2.07E+19	m^3	
$M_{Core\ Initial} = M_{IC} + M_{OC}$	9.19E+20	kg	
$M_{Mantle\ Initial} = M_{LM} + M_{LC}$	7.26E+22	kg	B19
$M_{Total\ Moon}$	7.35E+22	kg	
$U_{Core\ Initial} = -3GM_{CI}^{\ 2}/(5R_{CI})$	-1.03E+26	J	
$M_{CI} - \rho_{MI}V_{CI}$	3.95E+20	kg	
$R_{EI}^{\ 2} - R_{CI}^{\ 2}$	2.79E+12	m^2	
$R_{EI}^{\ 5} - R_{CI}^{\ 5}$	1.43E+31	m^5	
$U_{Mantle\ Initial}$	-1.27E+29	J	M17
$U_{Moon\ Initial} = U_{CI} + U_{MI}$	-1.27E+29	J	Result

Table 3 - Potential Energy Difference			
Parameter	Amount	Units	Ref
$U_{Moon\ Initial}$	-1.27E+29	J	F20
$U_{Moon\ Current}$	-1.26E+29	J	F20
$\Delta U_{Expansion} = U_{EC} - U_{EI}$	1.70E+27	J	Result

Table 4 - Lunar Thermal Expansion Ratios			
Parameter	**Amount**	**Units**	**Ref**
$R_{Moon\ Current}/R_{Moon\ Initial}$	1.0203	m/m	B8,F6
$A_{Moon\ Current}/A_{Moon\ Initial} = (R_{MC}/R_{MI})^2$	1.0411	m^2/m^2	B8,F6
$V_{Moon\ Current}/V_{Moon\ Initial} = (R_{MC}/R_{MI})^3$	1.0622	m^3/m^3	B8,F6
Sum of Crack Widths = $2\pi(R_{MC} - R_{MI})$	217,398.21	m	Result
Sum of Crack Areas = $4\pi(R_{MC}^2 - R_{MI}^2)$	1.50E+12	m^2	Result

Sheet 3 Explanatory Notes — Overall Heat Balance

Here we calculate the heat available from accelerated decay, after subtracting the small amount needed to provide expansion against gravity. Unlike the parallel set of calculations for the Earth, there is more than enough energy to heat the Moon up to its currently estimated core temperature in the range 1600-1700 K. There is thus a need to account for the excess heat available via various loss channels, such as radiation, loss of water vapour and partial melting of lunar mantle material. Drake et al (**18**) suggested that all radionuclides could have been quantitatively extracted from the mantle into what has become the current crust. This could have selectively heated this material to nearly its boiling point (**Table 4**) before delivering it to the surface, from which radiative heat transfer (**Table 6**) can be estimated. It is not essential for the whole lunar surface to be molten, as the vigorous volcanic processes produced by accelerated decay would atomise the hot lava into fine droplets, which would have increased the effective surface area dramatically. The initial breakthrough of lava would have been through deep vertical channels near weak points in the lunar surface and would have happened at a catastrophic rate, creating mountains as high as the current crustal thickness. This could account for the greater radiometric "ages" of highland regions. The boiling point of crustal lava has been estimated from that for $\mathbf{SiO_2}$ and the melting point for $\mathbf{Mg_2SiO_4}$, the chief constituent of the mantle. The ratio of boiling to melting point has been assumed to be the same for both minerals, as this is true of the high-melting metals considered in **Table 4**. The prospect of heating minerals to their boiling points opens the door to evaporative heat loss, here estimated in **Table 10**, after that due to sensible heating of the mantle (**Table 7**), boiling of water (**Table 8**) and partial melting of the mantle (**Table 9**). The estimate for initial heating of the eventual crustal material (**Table 5**) is not included in the proposed heat balance (**Table 11**), as its heat would eventually find a place somewhere within the sinks indentified in **Tables 6** to **10**. References for input data are highlighted in yellow, with cited sources in the **References** table. If data is taken from another cell in the same sheet, the cell reference is shown, highlighted in cyan. If it is from another sheet, the sheet number appears before the cell reference. Along with key results, a magenta highlight indicates achievement of the goal of an initially ambient temperature before thermal expansion, using trial values of initial lunar radii.

References

No.	Source
1	Doin M P & Fleitout L, **Thermal evolution of the oceanic lithosphere: an alternative view**, Elsevier, Earth and Planetary Science Letters, 142, 121-136 (1996)
2	https://en.wikipedia.org/wiki/Mantle_(geology)
3	https://en.wikipedia.org/wiki/Outer_core
4	Aitta A, **Iron melting curve with a tricritical point**, A.Aitta@damtp.cam.ac.uk
5	https://en.wikipedia.org/wiki/Iron
6	Kandpal D & Gupta B R K, **Analysis of thermal expansivity of iron (Fe) metal at ultra high temperature and pressure**, Indian Academy of Sciences, Pramana Journal of Physics, Vol. 68, No. 1, 129-164 (2007)
7	Desai P D, **Thermodynamic Properties of Iron and Silicon**, J Phys. Chem. Ref. Data, Vol. 15, No. 3 (1986)
8	https://en.wikipedia.org/wiki/Internal_structure_of_the_Moon
9	https://en.wikipedia.org/wiki/Tungsten
10	http://ltmlab.fr/wiki-materials/index.php?title=Silicon_dioxide_-_SiO2
11	https://en.wikipedia.org/wiki/Forsterite
12	https://en.wikipedia.org/wiki/Boltzmann_constant
13	https://en.wikipedia.org/wiki/Planck_constant
14	https://en.wikipedia.org/wiki/Speed_of_light
15	https://en.wikipedia.org/wiki/Stefan-Boltzmann_constant
16	https://en.wikipedia.org/wiki/Stefan-Boltzmann_law
17	https://en.wikipedia.org/wiki/Water_(data_page)#Water/steam_equilibrium_properties
18	Stacey F D & Davis P M, **Physics of the Earth**, 4th Edition, Cambridge University Press (2008)
19	Stacey F D & Davis P M, **Physics of the Earth**, 4th Edition, Cambridge University Press (2008)
20	Drake M J, Lowe J P, Righter K, Zuber M T & Clark P E, **Uranium in the Lunar Crust: Implications for Lunar Origin and Evolution**, Proc. 61st Annual Meteoritical Society Meeting, 5174.pdf (1998)

Table 1 - Energy Supply			
Parameter	**Amount**	**Units**	**Ref**
$E_{Grand\ Total\ Decay}$	1.16E+29	J	1.J37
$\Delta U_{Expansion}$	1.70E+27	J	2.F26
$\Delta U_E/E_{GTD}$	1.5%	J	
$E_{Available\ as\ Heat} = E_{GTD} - \Delta U_E$	1.15E+29	J	Result

Table 2 - Outer Core Expansion			
Parameter	**Amount**	**Units**	**Ref**
$M_{Outer\ Core}$	4.63E+20	kg	2.B18
$\rho_{Outer\ Core\ Current}$	5000	kg/m^3	2.B10
$v_{Outer\ Core\ Current} = 1/\rho_{OCC}$	2.00E-04	m^3/kg	
$V_{Outer\ Core\ Initial}$	9.02E+16	m^3	2.F9,B15
$\rho_{Outer\ Core\ Initial} = M_{OC}/V_{OCI}$	5134	kg/m^3	
$v_{Outer\ Core\ Initial} = 1/\rho_{OCI}$	1.95E-04	m^3/kg	
$\Delta v_{Outer\ Core} = v_{MC} - v_{MI}$	5.20E-06	m^3/kg	
Δv_{Fusion}	6.70E-08	m^3/mol	4
A_{Fe}	5.58E-02	kg/mol	5
$\Delta v_{Fusion} = \Delta v_F/A_{Fe}$	1.20E-06	m^3/kg	
$\Delta v_{Fusion}/v_{Outer\ Core\ Current}$	0.60%	m^3/kg	
$\Delta v_{Temperature} = \Delta v_{OC} - \Delta v_F$	4.00E-06	m^3/kg	
$\beta_{Outer\ Core}$	1.50E-05	$m^3m^{-3}K^{-1}$	6
$\Delta T_{Outer\ Core} = \Delta v_{OC}/(\beta_{OC}v_{OC})$	1352	K	
$T_{Outer\ Core\ Current}$	1650	K	8
$T_{Outer\ Core\ Initial} = T_{OCC} - \Delta T_{OC}$	298	K	Goal
Δh_{Fusion}	5.00E+05	J/kg	7
ΔH_{Fusion}	2.32E+26	J	
$C_{Outer\ Core}$	46	$Jmol^{-1}K^{-1}$	
$C_{Outer\ Core} = C_{OC}/A_{Fe}$	824	$Jkg^{-1}K^{-1}$	
$\Delta H_{Temperature} = C_{OC}\Delta T_{OC}M_{OC}$	5.16E+26	J	
$\Delta H_{Outer\ Core\ Overall} = \Delta H_T + \Delta H_F$	7.47E+26	J	

Table 3 - Mantle Expansion			
Parameter	**Amount**	**Units**	**Ref**
$\rho_{Mantle\ Initial}$	3535	kg/m^3	**2.F8**
$v_{Mantle\ Initial} = 1/\rho_{MI}$	2.83E-04	m^3/kg	
$\rho_{Mantle\ Current} = M_M/V_{MC}$	3399	kg/m^3	**2.B11**
$v_{Mantle\ Current} = 1/\rho_{MC}$	2.94E-04	m^3/kg	
$\Delta v_{Mantle} = v_{MC} - v_{MI}$	1.14E-05	m^3/kg	
β_{Mantle}	3.85E-05	$m^3m^{-3}K^{-1}$	**1**
$\Delta T_{Mantle\ Heating} = \Delta v_M/(\beta_M v_M)$	1026	K	
$T_{Mantle\text{-}Crust\ Current}$	1000	K	**Trial**
$T_{Core\text{-}Mantle\ Current}$	1650	K	**F18**
$T_{Mantle\ Current\ Average} = (T_{MCC} + T_{CMC})/2$	1325	K	
$T_{Mantle\ Initial} = T_{MCA} - \Delta T_{MH}$	299	K	**Goal**

Table 4 - Estimation of Lunar Lava Temperature			
Parameter	**Amount**	**Units**	**Ref**
Iron - $T_{Melting}$	1811	K	5
Iron - $T_{Boiling}$	3134	K	5
Iron - T_B/T_M	1.731	K/K	
Tungsten - $T_{Melting}$	3695	K	9
Tungsten - $T_{Boiling}$	6203	K	9
Tungsten - T_B/T_M	1.679	K/K	
Silicon Dioxide - $T_{Melting}$	1976	K	10
Silicon Dioxide - $T_{Boiling}$	2863	K	10
Silicon Dioxide - T_B/T_M	1.449	K/K	
Forsterite - $T_{Melting}$	2163	K	11
Forsterite - $T_B/T_M = T_B/T_M(SiO_2)$	1.449	K/K	11
Forsterite - $T_{Boiling} = T_M(T_B/T_M)$	3134	K	
Target - $T_S = [T_B(SiO_2) + T_B(Mg_2SiO_4)]/2$	2998	K	Result

Table 5 - Energy Requirements to Heat Crust			
Parameter	**Amount**	**Units**	**Ref**
Target Surface Temperature - T_S	2998	K	B40
$M_{Lunar\ Crust}$	6.40E+21	kg	1.B20
$\Delta H_{Crust\ Heating} = C_M M_{LC}(T_S - T_{MI})$	1.94E+28	J	Result

Table 6 - Radiation Heat Loss			
Parameter	**Amount**	**Units**	**Ref**
Boltzmann Constant - k_B	1.38E-23	J/K	12
Planck Constant - h	6.63E-34	Js	13
Speed of Light - c	3.00E+08	m/s	14
Stefan-Boltzmann - $\sigma = 2\pi^5 k_B^4/(15h^3c^2)$	5.67E-08	$Jm^{-2}s^{-1}K^{-1}$	15
Overall Lunar Radius - R_O	1.74E+06	m	1.B4
Lunar Surface Area - $A_L = 4\pi R_O^2$	3.79E+13	m^2	
Fraction of Surface Covered by Lava - F_{SCL}	30%	m^2/m^2	Trial
Atomisation Area Increase Factor - F_{AAI}	500%	m^2/m^2	Trial
Effective Radiating Area - $A_E = A_L F_{SCL} F_{AAI}$	5.69E+13	m^2	
Trial Surface Temperature - T_S	2998	K	B40
Maximum Radiated Power - $P_M = \sigma A_E T_S^4$	2.61E+20	W	16
Timescale for Radiation - t_R (1 year)	3.16E+07	s	Flood
Radiated Energy Estimate - $\Delta H_R = P_M t_R$	8.23E+27	J	Result

Table 7 - Energy Requirements to Heat Mantle			
$\Delta T_{Mantle\ Heating}$	1026	K	B17
C_{Mantle}	1124	$Jkg^{-1}K^{-1}$	1
$M_{Lunar\ Mantle}$	6.62E+22	kg	1.B19
$\Delta H_{Mantle\ Heating} = C_M \Delta T_{MH} M_{LM}$	7.63E+28	J	Result

Table 8 - Cooling Capacity of Water-Steam Transition			
Parameter	**Amount**	**Units**	**Ref**
Latent Heat at 0°C - $\Delta h_{Steam-Water}$	2.50E+06	J/kg	17
M_{Water}/M_{Moon}	8%	kg/kg	Trial
M_{Moon}	7.35E+22	$Jkg^{-1}K^{-1}$	1.B19
Cooling Capacity - $\Delta H_{SW} = \Delta h_{SW} M_{Water}$	1.47E+28	J	Result

Table 9 - Cooling Capacity of Partial Melting			
Parameter	**Amount**	**Units**	**Ref**
Heat of Fusion - Δh_{Fusion}	4.20E+05	J/kg	16
Melt Fraction - F_{Melt}	30%	kg/kg	Trial
$M_{Lunar\ Mantle}$	6.62E+22	kg	B7
Cooling Capacity - $\Delta H_F = \Delta h_F M_{LM} F_M$	8.34E+27	J	Result

Table 10 - Cooling Capability of Silica Vapourisation			
Parameter	**Amount**	**Units**	**Ref**
Latent Heat of Silica Vapour - $\Delta h_{LSV}(SiO_2)$	143.4	kcal/mol	18
$\Sigma A(SiO_2)$	6.00E-02	kg/mol	
Energy Units Conversion Factor	4184	J/kcal	
$\Delta h_{LSV}(SiO_2)$	1.00E+07	J/kg	
Fraction of Current Crust Boiling - F_{CCB}	35%	kg/kg	Trial
$M_{Lunar\ Crust}$	6.40E+21	kg	B45
Cooling Capacity - $\Delta H_{LV} = \Delta h_{LSV} M_{LC} F_{CCB}$	2.24E+28	J	Result

Table 11 - Proposed Energy Balance for Mantle			
Parameter	**Amount**	**Units**	**Ref**
$E_{Available\ as\ Heat}$	1.15E+29	J	B7
$\Delta H_{Total} = \Sigma\Delta H_{MH + R + SW + F + LV}$	1.30E+29	J	
$E_{AH}/\Delta H_T$	88.2%	J/J	Result

APPENDIX B – THERMAL CALCULATIONS OF MARS

Sheet 1 Explanatory Notes — Accelerated Decay

Here we calculate the energy available on the planet Mars from accelerated nuclear decay equivalent to that which would emerge over the conventionally dated age of the Earth. We consider the major radionuclides to be **Uranium-235**, **Uranium-238**, **Thorium-232** and **Potassium-40** with principal decay modes known to be **Alpha** for the heavy isotopes and **Beta** for potassium. In the absence of data to the contrary, the relative abundances of these isotopes have been assumed to be the same as those on Earth, with data on Thorium being available from a model for bulk Mars (**2**), taken from measurements of surface Thorium concentrations and the inference that this applies through the whole Martian crust, which is also assumed to contain the same current total mass of radionuclides as that in the now-depleted mantle. This results in a total decay energy just under 1/3 that calculated for Earth, which which is 9 times more massive than Mars. This would result in Mars being more intensely heated that Earth during the period of accelerated decay, even though Earth's mass can support higher internal temperatures. If the inferred concentrations are correct, then Mars needs to have radiated much of its heat into space, just as was found for the Moon (**12**). The excess is more severe for Mars than the Moon but a longer cooling time could be allowed (**Sheet 3**). References for input data are highlighted in yellow, with cited sources in the above table. If data is taken from another cell in the same sheet, the cell reference is shown, highlighted in cyan. If it is from another sheet, the sheet number appears before the cell reference. Key result fields are highlighted to the right in magenta.

References

No.	Source
1	https://en.wikipedia.org/wiki/Mars
2	Taylor G J & Boynton W V, **Global Concentrations of Thorium, Potassium and Chlorine: Implications for Martian Bulk Composition**, Proc. 40th Lunar and Planetary Science Conference, 1411.pdf (2009)
3	Zuber M T, **The Crust and Mantle of Mars**, Nature, Vol 412, 220-227 (12 July 2001)
4	https://en.wikipedia.org/wiki/Uranium-235#Natural_decay_chain
5	https://arxiv.org/abs/hep-ph/0409152v1
6	Meslin P Y, Hamara D K, Boynton W V, Sabroux J C & Gasnault O, **Analysis of Uranium and Thorium Lines in Mars Odyssey Gamma Spectra and Refined Mapping of Atmospheric Radon**, Proc. 43rd Lunar and Planetary Science Conference, 2852.pdf (2012)
7	https://en.wikipedia.org/wiki/Electron
8	https://en.wikipedia.org/wiki/Avogadro_constant
9	https://en.wikipedia.org/wiki/Abundances_of_the_elements_(data_page)
10	https://en.wikipedia.org/wiki/Potassium-40
11	https://en.wikipedia.org/wiki/Age_of_the_Earth
12	Stenberg D B & Silvester R S, **Stenberg-Silvester Model Calculations - Moon 2019-03-06**, Excel file available from rssconsultancy@aol.com or dnstnbrg@hotmail.com (6 March 2019)

Table 1 - Crust Mantle and Core Masses			
Parameter	**Amount**	**Units**	**Ref**
R_{Planet}	3.39E+06	m	1
t_{Crust}	5.70E+04	m	2
$R_{Mantle} = R_{Pl} - t_{Cr}$	3.33E+06	m	B4,5
$d_{Mantle} = t_{Mantle} + t_{Cr}$	1.76E+06	m	2
$R_{Core} = R_{Pl} - d_{Ma}$	1.63E+06	m	B4,7
$V_{Planet} = 4\pi R_{Pl}^{3}/3$	1.63E+20	m^3	B4
$V_{Crust} = 4\pi(R_{Pl} - t_{Cr}/2)^{2}t_{Cr}$	8.09E+18	m^3	B4,5
$V_{Mantle} = 4\pi(R_{Ma}^{3} - R_{Co}^{3})/3$	1.37E+20	m^3	B6,8
$V_{Core} = 4\pi(R_{Co}^{3})/3$	1.81E+19	m^3	B8
$\rho_{Average} = M_{Pl}/V_{Pl}$	3934	kg/m^3	B17,9
ρ_{Crust}	2900	kg/m^3	3
ρ_{Mantle}	3500	kg/m^3	3
$\rho_{Core} = M_{Co}/V_{Co}$	7675	kg/m^3	B17,9
M_{Planet}	6.42E+23	kg	1
$M_{Crust} = \rho_{Cr}V_{Cr}$	2.35E+22	kg	B14,10
$M_{Mantle} = \rho_{Ma}V_{Ma}$	4.79E+23	kg	B15,11
$M_{Core} = M_{Pl} - M_{Cr} - M_{Ma}$	1.39E+23	kg	

Table 2 - Decay Specific Energy Units Conversion			
Parameter	**Amount**	**Units**	**Ref**
$E_{Specific}(^{235}U)$	4.68E+07	eV/atom	4
$E_{Specific}(^{238}U)$	5.17E+07	eV/atom	5
$E_{Specific}(^{232}Th)$	4.27E+07	eV/atom	5
$E_{Specific}(^{40}K)$	1.32E+06	eV/atom	5
q(electron)	1.60E-19	J/eV	7
$N_{Avogadro}$	6.02E+23	atoms/mol	8
$A(^{235}U)$	2.35E-01	kg/mol	
$A(^{238}U)$	2.38E-01	kg/mol	
$A(^{232}Th)$	2.32E-01	kg/mol	
$A(^{40}K)$	4.00E-02	kg/mol	
$E_{Specific}(^{235}U) = E_S(^{235}U)qN_A/A(^{235}U)$	1.92E+13	J/kg	
$E_{Specific}(^{238}U) = E_S(^{238}U)qN_A/A(^{238}U)$	2.10E+13	J/kg	
$E_{Specific}(^{232}Th) = E_S(^{232}Th)qN_A/A(^{232}Th)$	1.78E+13	J/kg	
$E_{Specific}(^{40}K) = E_S(^{40}K)qN_A/A(^{40}K)$	3.18E+12	J/kg	

Table 3 - Current Radioisotope Inventories			
Parameter	**Amount**	**Units**	**Ref**
$[^{232}Th]_{Mantle\ Mars}$	2.80E-08	kg/kg	2
$([^{232}Th]_M/[U]_M)_{Earth}$	4.00	kg/kg	5,6
$([U]_M/[^{232}Th]_M)_{Earth}$	25%	kg/kg	F5
$[U]_{Mantle\ Mars} = [^{232}Th]_{MM}([U]_M/[^{232}Th]_M)_E$	7.00E-09	kg/kg	F4,6
$[K]_{Mantle\ Mars}$	1.50E-04	kg/kg	2
$([^{40}K]/[K])_{Earth}$	1.20E-04	kg/kg	10
$[^{40}K]_{Mantle\ Mars} = [K]_{MM}([^{40}K]/[K])_E$	1.80E-08	kg/kg	F8,9
$M_{Mantle\ Mars}(U) = M_{Ma}[U]_{MM}$	3.35E+15	kg	B19,F7
$M_{Mantle\ Mars}(^{232}Th) = M_{Ma}[^{232}Th]_{MM}$	1.34E+16	kg	B19,F4
$M_{Mantle\ Mars}(^{40}K) = M_{Ma}[^{40}K]_{MM}$	8.62E+15	kg	B19,F10
$M_{Crust\ Mars}(U) = M_{MM}(U)$	3.35E+15	kg	2
$M_{Crust\ Mars}(^{232}Th) = M_{MM}(^{232}Th)$	1.34E+16	kg	2
$M_{Crust\ Mars}(^{40}K) = M_{MM}(^{40}K)$	8.62E+15	kg	2
$[U]_{Crust\ Mars} = M_{CM}(U)/M_{Cr}$	1.43E-07	kg/kg	F14,B18
$[^{232}Th]_{Crust\ Mars} = M_{CM}(^{232}Th)/M_{Cr}$	5.72E-07	kg/kg	F15,B18
$[^{40}K]_{Crust\ Mars} = M_{CM}(^{40}K)/M_{Cr}$	3.68E-07	kg/kg	F16,B18
$M_{Total}(U) = M_C(U) + M_M(U)$	6.71E+15	kg	F14,11
$M_{Total}(^{232}Th) = M_C(^{232}Th) + M_M(^{232}Th)$	2.68E+16	kg	F15,12
$M_{Total}(^{40}K) = M_C(^{40}K) + M_M(^{40}K)$	1.72E+16	kg	F16,13
$[^{235}U]/[U]$	0.72%	kg/kg	4
$M_{Total}(^{235}U) = M_T(U)[^{235}U]/[U]$	4.83E+13	kg	F23,20
$[^{238}U]/[U]$	99.27%	kg/kg	4
$M_{Total}(^{238}U) = M_T(U)[^{238}U]/[U]$	6.66E+15	kg	F25,20

Table 3 - Current Radioisotope Inventories			
Parameter	**Amount**	**Units**	**Ref**
$[^{232}Th]_{Bulk} = M_T(^{232}Th)/(M_{Cr} + M_{Ma})$	5.34E-08	**kg/kg**	**2**
$[K]_{Bulk} = ([K]/[^{40}K])_E M_T(^{40}K)/(M_{Cr+Ma})$	2.86E-04	**kg/kg**	**2**

Table 4 - Accelerated Decay Energy			
Parameter	**Amount**	**Units**	**Ref**
Uniformitarian Decay Time (t_{Total})	4.54E+09	year	11
$t_{Half}(^{235}U)$	7.04E+08	year	4
$t_{Half}(^{238}U)$	4.47E+09	year	5
$t_{Half}(^{232}Th)$	1.40E+10	year	5
$t_{Half}(^{40}K)$	1.28E+09	year	5
$t_{Total}/t_{Half}(^{235}U)$	6.45	year/year	
$t_{Total}/t_{Half}(^{238}U)$	1.02	year/year	
$t_{Total}/t_{Half}(^{232}Th)$	0.32	year/year	
$t_{Total}/t_{Half}(^{40}K)$	3.55	year/year	
$2^{tT/tHU235} = 2\text{^}[t_{Total}/t_{Half}(^{235}U)]$	87.47	kg/kg	
$2^{tT/tHU238} = 2\text{^}[t_{Total}/t_{Half}(^{238}U)]$	2.02	kg/kg	
$2^{tT/tHTh232} = 2\text{^}[t_{Total}/t_{Half}(^{232}Th)]$	1.25	kg/kg	
$2^{tT/tHK40} = 2\text{^}[t_{Total}/t_{Half}(^{40}K)]$	11.69	kg/kg	
$M_{Current}(^{235}U)$	4.83E+13	kg	F28
$M_{Current}(^{238}U)$	6.66E+15	kg	F30
$M_{Current}(^{232}Th)$	2.68E+16	kg	F25
$M_{Current}(^{40}K)$	1.72E+16	kg	F26
$M_{Initial}(^{235}U) = 2^{tT/tHU235}M_C(^{235}U)$	4.22E+15	kg	
$M_{Initial}(^{238}U) = 2^{tT/tU238}M_C(^{238}U)$	1.35E+16	kg	
$M_{Initial}(^{232}Th) = 2^{tT/tHTh232}M_C(^{232}Th)$	3.36E+16	kg	
$M_{Initial}(^{40}K) = 2^{tT/tHK40}M_C(^{40}K)$	2.02E+17	kg	
$\Delta M(^{235}U) = M_I(^{235}U) - M_C(^{235}U)$	4.18E+15	kg	
$\Delta M(^{238}U) = M_I(^{238}U) - M_C(^{238}U)$	6.81E+15	kg	

Table 4 - Accelerated Decay Energy			
Parameter	**Amount**	**Units**	**Ref**
$\Delta M(^{232}Th) = M_I(^{232}Th) - M_C(^{232}Th)$	6.76E+15	kg	
$\Delta M(^{40}K) = M_I(^{40}K) - M_C(^{40}K)$	1.84E+17	kg	
$E_{Specific}(^{235}U)$	1.92E+13	J/kg	B26
$E_{Specific}(^{238}U)$	2.10E+13	J/kg	B27
$E_{Specific}(^{232}Th)$	1.78E+13	J/kg	B28
$E_{Specific}(^{40}K)$	3.18E+12	J/kg	B29
$E_{Total}(^{235}U) = E_S(^{235}U)\Delta M(^{235}U)$	8.02E+28	J	
$E_{Total}(^{238}U) = E_S(^{238}U)\Delta M(^{238}U)$	1.43E+29	J	
$E_{Total}(^{232}Th) = E_S(^{232}Th)\Delta M(^{232}Th)$	1.20E+29	J	
$E_{Total}(^{40}K) = E_S(^{40}K)\Delta M(^{40}K)$	5.87E+29	J	
$E_{Grand\ Total\ Decay}$	9.30E+29	J	Result

Sheet 2 Explanatory Notes — Gravitational Energy

Here we calculate the gravitational potential difference that would be met by the decay-heat-induced expansion of Mars, which is currently divided into layers with the labels **Core**, **Mantle** and **Crust**, as we had not enough information to be able to identify the dimensions of separate inner and outer cores. As it is assumed to be initially cool and solid, with a homogeneous mantle, Mars is initially partitioned into **Core Initial** and **Mantle Initial**, with trial values for initial radii. Densities emerging from these trials are then fed into **Sheet 3** for a calculation of initial temperature. The trial values are then adjusted to yield an initial temperature of order 300 K (27°C). There are, listed and derived above, formulae used to calculate potential energy for spherically symmetric bodies. References for input data are highlighted in yellow, with cited sources in the **References** table. If data is taken from another cell in the same sheet, the cell reference is shown, highlighted in cyan. If it is from another sheet, the sheet number appears before the cell reference. Along with key results, a magenta highlight indicates a trial input, such as initial surface and core radii, that would support the initially ambient temperature before thermal expansion.

References

No.	Source
1	https://en.wikipedia.org/wiki/Gravitational_constant

Sheet 3 Explanatory Notes — Overall Heat Balance

Here we calculate the heat available from accelerated decay, after

Expansion Energy Formulae
Initial Conditions
$dU_{Core\ Initial} = -GMdM/R = -GM4\pi\rho R^2dR/R = -GM4\pi\rho RdR = -G(4\pi)^2\rho^2R^4dR/3$
$U_{Core\ Initial} = -G(4\pi)^2\rho_{CI}^2R_{CI}^5/15 = 3GM_{CI}^2/(5R_{CI})$
$dU_{Mantle\ Initial} = -GMdM/R = -G[M_{CI} + \rho_{MI}(4\pi R^3/3 - V_{CI})]\rho_{MI}4\pi RdR$
$U_{Mantle\ Initial} = -G[2\pi\rho_{MI}(M_{CI} - \rho_{MI}V_{CI})(R_{MI}^2 - R_{CI}^2) + 16\pi^2\rho_{MI}^2(R_{MI}^5 - R_{CI}^5)/15]$
$U_{Mantle\ Initial} = -G\rho_{MI}[2\pi(M_{CI} - \rho_{MI}V_{CI})(R_{MI}^2 - R_{CI}^2) + 16\pi^2\rho_{MI}(R_{MI}^5 - R_{CI}^5)/15]$
Current Conditions
$U_{Core} = -3GM_{Co}^2/(5R_{Co})$
$U_{Mantle} = -G[2\pi\rho_{Ma}(M_{Co} - \rho_{Ma}V_{Co})(R_{Ma}^2 - R_{Co}^2) + 16\pi^2\rho_{Ma}^2(R_{Ma}^5 - R_{Co}^5)/15]$
$U_{Crust} = -G[2\pi\rho_{Cr}(M_{Co+Ma} - \rho_{Cr}V_{Co+Ma})(R_{Cr}^2 - R_{Ma}^2) + 16\pi^2\rho_{Cr}^2(R_{Cr}^5 - R_{Ma}^5)/15]$
InTerms of Mass (Simple Core-Mantle System)
$U_{Mantle} = -G\rho_M[2\pi(M_C - \rho_MV_C)(R_M^2 - R_C^2) + 16\pi^2\rho_M(R_M^5 - R_C^5)/15]$
$U_{Mantle} = -GM_M[2\pi(M_C - \rho_MV_C)(R_M^2 - R_C^2) + 16\pi^2\rho_M(R_M^5 - R_C^5)/15]/[4\pi(R_M^3 - R_C^3)/3]$
$U_{Mantle} = -GM_M[(M_C - \rho_MV_C)(R_M^2 - R_C^2) + 8\pi\rho_M(R_M^5 - R_C^5)/15]/[2(R_M^3 - R_C^3)/3]$
$U_{Mantle} = -3GM_M[(M_C(R_M^2 - R_C^2) + \rho_M(4\pi R_C^3/3)(R_C^2 - R_M^2) + 8\pi\rho_M(R_M^5 - R_C^5)/15]/[2(R_M^3 - R_C^3)]$
$U_{Mantle} = -3GM_M[(M_C(R_M^2 - R_C^2) + (4\pi\rho_M/3)\{R_C^3(R_C^2 - R_M^2) + 2(R_M^5 - R_C^5)/5\}]/[2(R_M^3 - R_C^3)]$
$U_{Mantle} = -3GM_M[(M_C(R_M^2 - R_C^2) + M_M\{R_C^3(R_C^2 - R_M^2) + 2(R_M^5 - R_C^5)/5\}/(R_M^3 - R_C^3)]/[2(R_M^3 - R_C^3)]$
$U_{Mantle} = -3GM_M[(M_C(R_M^2 - R_C^2) + (M_M/5)(5R_C^5 - 5R_C^3R_M^2 + 2R_M^5 - 2R_C^5)/(R_M^3 - R_C^3)]/[2(R_M^3 - R_C^3)]$
$U_{Mantle} = -(3GM_M/2)\{(M_C(R_M^2 - R_C^2) + (M_M/5)(3R_C^5 - 5R_C^3R_M^2 + 2R_M^5)/(R_M^3 - R_C^3)\}/(R_M^3 - R_C^3)$

Table 1 - Current Potential Energy			
Parameter	**Amount**	**Units**	**Ref**
G	6.67E-11	$m^3kg^{-1}s^{-2}$	**1**
R_{Core}	1.63E+06	m	**1.B8**
R_{Mantle}	3.33E+06	m	**1.B6**
R_{Crust}	3.39E+06	m	**1.B4**
ρ_{Core}	7675	kg/m^3	**1.B16**
ρ_{Mantle}	3500	kg/m^3	**1.B15**
ρ_{Crust}	2900	kg/m^3	**1.B14**
V_{Core}	1.81E+19	m^3	**1.B12**
V_{Mantle}	1.37E+20	m^3	**1.B11**
V_{Crust}	8.09E+18	m^3	**1.B10**
M_{Core}	1.39E+23	kg	**1.B20**
M_{Mantle}	4.79E+23	kg	**1.B19**
M_{Crust}	2.35E+22	kg	**1.B18**
$U_{Core} = -3GM_{Co}^2/(5R_{Co})$	-4.75E+29	J	**I14**
$M_{Co} - \rho_{Ma}V_{Co}$	7.57E+22	kg	
$R_{Ma}^2 - R_{Co}^2$	8.45E+12	m^2	
$R_{Ma}^5 - R_{Co}^5$	4.00E+32	m^5	
U_{Mantle}	-4.38E+30	J	**I15**
$M_{Co+Ma} - \rho_{Cr}V_{Co+Ma}$	1.69E+23	kg	
$R_{Cr}^2 - R_{Ma}^2$	3.83E+11	m^2	
$R_{Cr}^5 - R_{Ma}^5$	3.64E+31	m^5	
U_{Crust}	-2.94E+29	J	**I16**
$U_{Mars\ Current} = U_{Co} + U_{Ma} + U_{Cr}$	**-5.15E+30**	J	**Result**

Table 2 - Initial Potential Energy			
Parameter	Amount	Units	Ref
G	6.67E-11	$m^3kg^{-1}s^{-2}$	B4
$R_{Core\ Initial}$	1.61E+06	m	Trial
$R_{Mantle\ Initial}$	3.32E+06	m	Trial
$\rho_{Core\ Initial} = M_{CI}/V_{CI}$	7884	kg/m^3	F11,9
$\rho_{Mantle\ Initial} = M_{MI}/V_{MI}$	3696	kg/m^3	F12,10
$V_{Core\ Initial} = 4\pi R_{CI}^3/3$	1.76E+19	m^3	F5
$V_{Mantle\ Initial} = 4\pi(R_{MI}^3 - R_{CI}^3)/3$	1.36E+20	m^3	F6,5
$M_{Core\ Initial} = M_{Co}$	1.39E+23	kg	B14
$M_{Mantle\ Initial} = M_{Ma} + M_{Cr}$	5.03E+23	kg	B15,16
$U_{Core\ Initial} = -3GM_{CI}^2/(5R_{CI})$	-4.80E+29	J	I9
$M_{CI} - \rho_{MI}V_{CI}$	7.39E+22	kg	
$R_{MI}^2 - R_{CI}^2$	8.43E+12	m^2	
$R_{MI}^5 - R_{CI}^5$	3.94E+32	m^5	
$U_{Mantle\ Initial}$	-4.75E+30	J	I11
$U_{Moon\ Initial} = U_{CI} + U_{MI}$	-5.23E+30	J	Result

Table 3 - Potential Energy Difference			
Parameter	Amount	Units	Ref
$U_{Mars\ Initial}$	-5.23E+30	J	F20
$U_{Mars\ Current}$	-5.15E+30	J	F20
$\Delta U_{Expansion} = U_{MC} - U_{MI}$	7.97E+28	J	Result

Table 4 - Martian Thermal Expansion Ratios			
Parameter	Amount	Units	Ref
$R_{Mars\ Current}/R_{Mars\ Initial}$	1.0202	m/m	B7,F6
$A_{Mars\ Current}/A_{Mars\ Initial} = (R_{MC}/R_{MI})^2$	1.0407	m^2/m^2	F28
$V_{Mars\ Current}/V_{Mars\ Initial} = (R_{MC}/R_{MI})^3$	1.0617	m^3/m^3	F28
Sum of Crack Widths = $2\pi(R_{MC} - R_{MI})$	421	km	Result
Sum of Crack Areas = $4\pi(R_{MC}^2 - R_{MI}^2)$	5,646,972	km^2	Result

subtracting the small amount needed to provide expansion against gravity. Unlike the parallel set of calculations for the Earth, there is excess energy to heat Mars up to its currently estimated mantle temperature of 1280-1600°C (**5**). There is thus a need to account for the excess heat available via various loss channels, such as radiation, loss of water vapour and partial melting of Martian mantle material. A similar calculation has been undertaken for the Moon (**17**), where the heat loss channels itemised here were identified. The excess on both Mars was not as severe as that on the Moon. Nevertheless, during accelerated decay, radionuclides could have been concentrated in the eventual crustal material, selectively heating it to its boiling point (**Table 4**) before delivering it to the surface, from which radiative heat transfer (**Table 6**) can be estimated. It is not essential for the whole Martian surface to be molten, as the vigorous volcanic processes produced by accelerated decay would atomise the hot lava into fine droplets, which would have increased the effective surface area dramatically. The initial breakthrough of lava would have been through deep vertical channels near weak points in the planetary surface and would have happened at a catastrophic rate, creating mountains as high as the current crustal thickness. The boiling point of crustal lava has been estimated from that for SiO_2 and the melting point for Mg_2SiO_4, the chief constituent of the mantle. The ratio of boiling to melting point has been assumed to be the same for both minerals, as this is true of the high-melting metals considered in **Table 4**. The prospect of heating minerals to their boiling points opens the door to evaporative heat loss, here estimated in **Table 10**, after that due to sensible heating of the mantle (**Table 7**), boiling of water (**Table 8**) and partial melting of the mantle (**Table 9**). The estimate for initial heating of the eventual crustal material (**Table 5**) is not included in the proposed heat balance (**Table 11**), as its heat would eventually find a place somewhere within the sinks indentified in **Tables 6** to **10**. References for input data are highlighted in yellow, with cited sources in the **References** table. If data is taken from another cell in the same sheet, the cell reference is shown, highlighted in cyan. If it is from another sheet, the sheet number appears before the cell reference. Along with key results, a magenta highlight indicates achievement of the goal of an initially ambient temperature before thermal expansion, using trial values of initial Martian radii. A time of order that of the Flood year, which would be isolated from observations of Martian surface disturbance, has been estimated for high-temperature radiative heat transfer from the planet. This also applies to the Moon.

References

No.	Source
1	Doin M P & Fleitout L, **Thermal evolution of the oceanic lithosphere: an alternative view**, Elsevier, Earth and Planetary Science Letters, 142, 121-136 (1996)
2	Aitta A, **Iron melting curve with a tricritical point**, A.Aitta@damtp.cam.ac.uk
3	https://en.wikipedia.org/wiki/Iron
4	Kandpal D & Gupta B R K, **Analysis of thermal expansivity of iron (Fe) metal at ultra high temperature and pressure**, Indian Academy of Sciences, Pramana Journal of Physics, Vol. 68, No. 1, 129-164 (2007)
5	Zuber M T, **The Crust and Mantle of Mars**, Nature, Vol 412, 220-227 (12 July 2001)
6	Desai P D, **Thermodynamic Properties of Iron and Silicon**, J Phys. Chem. Ref. Data, Vol. 15, No. 3 (1986)
7	https://en.wikipedia.org/wiki/Tungsten
8	http://ltmlab.fr/wiki-materials/index.php?title=Silicon_dioxide_-_SiO2
9	https://en.wikipedia.org/wiki/Forsterite
10	https://en.wikipedia.org/wiki/Boltzmann_constant
11	https://en.wikipedia.org/wiki/Planck_constant
12	https://en.wikipedia.org/wiki/Speed_of_light
13	https://en.wikipedia.org/wiki/Stefan-Boltzmann_constant
14	https://en.wikipedia.org/wiki/Stefan-Boltzmann_law
15	https://en.wikipedia.org/wiki/Water_(data_page)#Water/steam_equilibrium_properties
16	Stacey F D & Davis P M, **Physics of the Earth**, 4th Edition, Cambridge University Press (2008)
17	Stenberg D B & Silvester R S, **Stenberg-Silvester Model Calculations - Moon 2019-03-06**, Excel file available from rssconsultancy@aol.com or dnstnbrg@hotmail.com (6 March 2019)

Table 1 - Energy Supply			
Parameter	**Amount**	**Units**	**Ref**
$E_{Grand\ Total\ Decay}$	9.30E+29	J	1.J37
$\Delta U_{Expansion}$	7.97E+28	J	2.F26
$\Delta U_E/E_{GTD}$	8.6%	J	
$E_{Available\ as\ Heat} = E_{GTD} - \Delta U_E$	8.50E+29	J	Result

Table 2 - Core Expansion			
Parameter	**Amount**	**Units**	**Ref**
$\rho_{Core\ Current}$	7675	kg/m^3	**2.B8**
$v_{Core\ Current} = 1/\rho_{CC}$	1.30E-04	m^3/kg	
$\rho_{Core\ Initial}$	7884	kg/m^3	
$v_{Core\ Initial} = 1/\rho_{CI}$	1.27E-04	m^3/kg	
$\Delta v_{Outer\ Core} = v_{MC} - v_{MI}$	3.47E-06	m^3/kg	
Δv_{Fusion}	6.70E-08	m^3/mol	**2**
A_{Fe}	5.58E-02	kg/mol	**3**
Molten Fraction - $F_M = V_{Molten}/V_{Core}$	87.5%	m^3/m^3	**Trial**
$\Delta v_{Fusion} = F_M \Delta v_F / A_{Fe}$	1.05E-06	m^3/kg	
$\Delta v_{Temperature} = \Delta v_C - \Delta v_F$	2.42E-06	m^3/kg	
β_{Core}	1.50E-05	$m^3m^{-3}K^{-1}$	**4**
$\Delta T_{Core} = \Delta v_C/(\beta_C v_C)$	1253	K	
$T_{Core\ Current}$	1553	K	**5**
$T_{Core\ Initial} = T_{CC} - \Delta T_C$	300	K	**Goal**
Δh_{Fusion}	5.00E+05	J/kg	**6**
$M_{Martian\ Core}$	1.39E+23	kg	**2.B14**
ΔH_{Fusion}	6.95E+28	J	
C_{Core}	46	$Jmol^{-1}K^{-1}$	
$C_{Core} = C_C/A_{Fe}$	824	$Jkg^{-1}K^{-1}$	
$\Delta H_{Temperature} = C_C \Delta T_C M_C$	1.44E+29	J	
$\Delta H_{Core\ Overall} = \Delta H_T + \Delta H_F$	2.13E+29	J	

Table 3 - Mantle Expansion			
Parameter	**Amount**	**Units**	**Ref**
$\rho_{Mantle\ Initial}$	3696	kg/m^3	**2.F8**
$v_{Mantle\ Initial} = 1/\rho_{MI}$	2.71E-04	m^3/kg	
$\rho_{Mantle\ Current}$	3500	kg/m^3	**2.B11**
$v_{Mantle\ Current} = 1/\rho_{MC}$	2.86E-04	m^3/kg	
$\Delta v_{Mantle} = v_{MC} - v_{MI}$	1.51E-05	m^3/kg	
β_{Mantle}	3.85E-05	$m^3m^{-3}K^{-1}$	**1**
$\Delta T_{Mantle\ Heating} = \Delta v_M/(\beta_M v_M)$	1413	K	
$T_{Mantle\text{-}Crust\ Current}$	1553	K	**5**
$T_{Core\text{-}Mantle\ Current}$	1873	K	**F16**
$T_{Mantle\ Current\ Average} = (T_{MCC} + T_{CMC})/2$	1713	K	
$T_{Mantle\ Initial} = T_{MCA} - \Delta T_{MH}$	300	K	**Goal**

Table 4 - Estimation of Lunar Lava Temperature			
Parameter	Amount	Units	Ref
Iron - $T_{Melting}$	1811	K	3
Iron - $T_{Boiling}$	3134	K	3
Iron - T_B/T_M	1.731	K/K	B26,25
Tungsten - $T_{Melting}$	3695	K	7
Tungsten - $T_{Boiling}$	6203	K	7
Tungsten - T_B/T_M	1.679	K/K	B29,28
Silicon Dioxide - $T_{Melting}$	1976	K	8
Silicon Dioxide - $T_{Boiling}$	2863	K	8
Silicon Dioxide - T_B/T_M	1.449	K/K	B32,31
Forsterite - $T_{Melting}$	2163	K	9
Forsterite - $T_B/T_M = T_B/T_M(SiO_2)$	1.449	K/K	9
Forsterite - $T_{Boiling} = T_M(T_B/T_M)$	3134	K	B35,34
Target - $T_S = [T_B(SiO_2) + T_B(Mg_2SiO_4)]/2$	2998	K	Result

Table 5 - Energy Requirements to Heat Crust			
Parameter	Amount	Units	Ref
Target Surface Temperature - T_S	2998	K	B40
$M_{Martian\ Crust}$	2.35E+22	kg	1.B20
$\Delta H_{Crust\ Heating} = C_M M_{LC}(T_S - T_{MI})$	7.12E+28	J	Result

Table 6 - Radiation Heat Loss			
Parameter	**Amount**	**Units**	**Ref**
Boltzmann Constant - k_B	1.38E-23	J/K	10
Planck Constant - h	6.63E-34	Js	11
Speed of Light - c	3.00E+08	m/s	12
Stefan-Boltzmann - $\sigma = 2\pi^5 k_B^4/(15h^3c^2)$	5.67E-08	$Jm^{-2}s^{-1}K^{-1}$	13
Overall Martian Radius - R_M	3.39E+06	m	1.B4
Martian Surface Area - $A_L = 4\pi R_O^2$	1.44E+14	m^2	
Fraction of Surface Covered by Lava - F_{SCL}	10%	m^2/m^2	Trial
Atomisation Area Increase Factor - F_{AAI}	500%	m^2/m^2	Trial
Effective Radiating Area - $A_E = A_L F_{SCL} F_{AAI}$	7.22E+13	m^2	
Trial Surface Temperature - T_S	2998	K	B37
Maximum Radiated Power - $P_M = \sigma A_E T_S^4$	3.31E+20	W	14
Timescale for Radiation - t_R (1 year)	3.16E+07	s	Flood
Radiated Energy Estimate - $\Delta H_R = P_M t_R$	1.04E+28	J	Result

Table 7 - Energy Requirements to Heat Mantle			
$\Delta T_{Mantle\ Heating}$	1413	K	B17
C_{Mantle}	1124	$Jkg^{-1}K^{-1}$	1
$M_{Martian\ Mantle}$	4.79E+23	kg	1.B15
$\Delta H_{Mantle\ Heating} = C_M \Delta T_{MH} M_{LM}$	7.61E+29	J	Result

Table 8 - Cooling Capacity of Water-Steam Transition			
Parameter	**Amount**	**Units**	**Ref**
Latent Heat at 0°C - $\Delta h_{Steam\text{-}Water}$	2.50E+06	J/kg	15
M_{Water}/M_{Mars}	2.9%	kg/kg	Trial
M_{Mars}	6.42E+23	$Jkg^{-1}K^{-1}$	1.B17
Cooling Capacity - $\Delta H_{SW} = \Delta h_{SW} M_{Water}$	4.65E+28	J	Result

Table 9 - Cooling Capacity of Partial Melting			
Parameter	**Amount**	**Units**	**Ref**
Heat of Fusion - Δh_{Fusion}	4.20E+05	J/kg	16
Melt Fraction - F_{Melt}	10%	kg/kg	Trial
$M_{Martian\ Mantle}$	4.79E+23	kg	B42
Cooling Capacity - $\Delta H_F = \Delta h_F M_{LM} F_M$	2.01E+28	J	Result

Table 10 - Cooling Capability of Silica Vapourisation			
Parameter	**Amount**	**Units**	**Ref**
Latent Heat of Silica Vapour - $\Delta h_{LSV}(SiO_2)$	143.4	kcal/mol	8
$\Sigma A(SiO_2)$	6.00E-02	kg/mol	
Energy Units Conversion Factor	4184	J/kcal	
$\Delta h_{LSV}(SiO_2)$	1.00E+07	J/kg	
Fraction of Current Crust Boiling - F_{CCB}	5%	kg/kg	Trial
$M_{Martian\ Crust}$	2.35E+22	kg	F29
Cooling Capacity - $\Delta H_{LV} = \Delta h_{LSV} M_{LC} F_{CCB}$	1.17E+28	J	Result

Table 11 - Proposed Energy Balance for Mantle			
Parameter	**Amount**	**Units**	**Ref**
$E_{Available\ as\ Heat}$	8.50E+29	J	B7
$\Delta H_{Total} = \Sigma\Delta H_{MH + R + SW + F + LV}$	8.50E+29	J	
$E_{AH}/\Delta H_T$	100.0%	J/J	Result

APPENDIX C – ACCELERATED NUCLEAR DECAY HEAT SUFFICIENT TO CAUSE MARE IMBRIUM

1. Heat Calculations

Decay of naturally occurring radioisotopes

Mare Imbrium	Value	Unit
Crater surface area	1.0297E+06	km^2
maria depth	1.3000E+00	km
maria density	2.7000E+12	kg/km^3
maria mass	3.6142E+18	kg

Nuclide	Half-life (yr)	Concentration	Present Mass	Original Mass	Energy (J/kg)	Total energy (J)
^{235}U	7.04E+08	2.16E-08	7.81E+10	6.56E+12	1.90E+13	1.23E+26
^{238}U	4.47E+09	2.98E-06	1.08E+13	2.16E+13	2.11E+13	2.29E+26
^{232}Th	1.41E+10	9.60E-06	3.47E+13	4.33E+13	1.77E+13	1.53E+26
^{40}K	1.25E+09	3.00E-06	1.08E+13	1.32E+14	3.21E+12	3.89E+26
Total						**8.94E+26**

2. Crater Size v. Energy

	Crater Diameter (m)	Est. Formation Energy (J)	3rd order polynomial	Power 1	Power 2
	3800	2.5E+18	-2.4E+20	1.1E+18	9.8E+17
	12000	1.6E+19	3.6E+20	4.5E+19	4.6E+19
	23000	3.1E+20	4.9E+20	3.7E+20	4.1E+20
	32000	1.0E+21	6.5E+20	1.1E+21	1.2E+21
	70000	1.5E+22	1.5E+22	1.4E+22	1.7E+22
	140000	2.1E+23	2.0E+23	1.3E+23	1.7E+23
Imbrium:	1146000	1.7E+26	1.7E+26	1.2E+26	2.0E+26

3 different Energy Estimates for Mare Imbrium Explosion, using 3 different extrapolations

PAGE SUMMARY: Crater size v crater energy